UNIVERSITÀ DEGLI STUDI DI PADOVA

UNIVERSITA' DEGLI STUDI DI PADOVA

Dipartimento di Ingegneria Industriale DII

Corso di Laurea Magistrale in Ingegneria Aerospaziale

DESIGN OF AN ADVANCED MICROTURBINE GENERATOR FOR LIGHT ELECTRIC AIRCRAFTS

Relatore: Ing. Francesco Barato

Studente: De Rossi Federico

Matricola: 1237231

Anno Accademico 2021/2022

Ai miei nonni

Abstract

The purpose of this thesis was to design and develop a microturbine generator to be used in light aircrafts, with the aim to power the electric motors generating the thrust to sustain the aircraft in cruise conditions. Having select as prototype plane the Airbus E-fan, various possible configurations for the gas turbine engine have been analysed, looking for innovative solutions and using components never introduced in aeronautical engines. For this reason, setups with intercooler and recuperator have been evaluated, choosing the one with both heat exchangers due to the numerous advantages in terms of specific fuel consumption, efficiencies, dimensions, and weight, that this configuration carries. The use of biofuels has been assessed, aiming for a strong reduction in emissions. Subsequently all the components have been designed and dimensioned opting, where possible, for cutting edge materials granting the best performance.

Sommario

Questo lavoro ha lo scopo di sviluppare un generatore a microturbina che possa essere applicato su aerei leggeri di piccola taglia, con lo scopo di produrre l'energia elettrica necessaria a generare la spinta per il sostentamento dell'aereo in condizioni di crociera. Dopo aver selezionato come velivolo su cui applicare il generatore, l'Airbus E-fan, si è passati ad analizzare varie configurazioni possibili per il motore, cercando soluzioni innovative ed utilizzando componenti mai introdotti in motori aeronautici. Per questo sono state valutate configurazioni con intercooler e recuperatore, scegliendo visti i vantaggi in termini di consumi specifici, di efficienze, di ingombri e pesi, la configurazione con entrambi gli scambiatori di calore. È stato valutato l'uso di biocarburanti con lo scopo di ridurre le emissioni nocive. A questo punto si è passati al design vero e proprio, dimensionando tutti i vari componenti optando per materiali all'avanguardia che consentissero di ottenere le prestazioni migliori possibili.

Ringraziamenti

Come prima cosa desidero ringraziare il professor Barato F. per avermi seguito e guidato in questa tesi con dedizione e voglia, aiutandomi ad esprimere al meglio le mie abilità.

Un immenso grazie ai miei genitori per avermi accompagnato e sostenuto in questo percorso, spronandomi sempre a seguire le mie passioni, e a mia sorella per essere stata un punto di riferimento al quale ispirarmi mentre crescevo. Non credo ci siano parole adatte per esprimere quanto vi sia riconoscente. Spero di avervi reso, almeno un po', orgogliosi di quello che ho fatto.

A Lorenzo, con cui ho avuto l'onore di condividere parte di questo percorso, Giovanni, Andrea, Cesare ed Alessandro. Dovunque saremo nel mondo il "comitato" sarà sempre con noi.
Ad Elena che da anni sopporta le mie lamentele e paranoie, un'amica così non si trova da nessuna parte.
A ciò che ne rimane della BSA. Pochi ma buoni, i migliori oserei dire.
Alla mia allenatrice Giovanna e a tutto il gruppo "Mezzofondisti si nasce", per aver sopportato tutte le mie assenze e per essere la mia valvola di sfogo da ormai sette anni. Non avrei mai potuto trovare un gruppo di allenamento migliore di questo.

Ci sono tante altre persone che vorrei ringraziare ma finirei per scrivere un'infinità di pagine. Perciò, mi limito a dire grazie a tutte le persone che sono state parte, anche solo per poco tempo, di questo mio percorso, perché ognuno di voi a suo modo ha contribuito a farmi diventare ciò che sono.

"Ad Astra, per Aspera"
Federico

Padova, 05 Aprile 2022

Table of contents

Index of Figures

Index of tables

Introduction

The aeronautic world is currently living its best period so far (if we do not count the last two years with the pandemic) since the Wright brothers made the first flight, with an extremely high passenger flow and number of flights rapidly increasing. Moving and travelling with a plane has become accessible to everyone, not only to richer people as it could be until the ’80. A report of the International Air Transport Association, IATA, of 2018 [1] describing the evolution of the market for the next decades, estimates that the number of passengers is set to double within 2037. Even though airliners and manufacturers have these huge incomes, the evolution and development of aircrafts have not followed the same path. It is true that a lot of new planes have been presented and built in the last years, but the technology used for aerodynamics and engines, apart for few changes, is the same used 50 years ago to develop and fly the first turbofans engines.

Focusing on the engine development, after the introduction of the aforementioned turbofan engines, derived from jet engines previously used in commercial and military planes in the sixties, there haven’t been significant changes or introduction of new and radical technologies or ideas allowing for a paradigm shift in the development of completely different engines.

The main manufactures, such as Rolls Royce and General Electric, focused on getting the best out such advanced engines, improving every single technical detail, introducing new advanced materials and increasing as much as possible the bypass ratio, in order to obtain significative performance and consumption improvements, even at the expense of the aerodynamics (massively ruined by these huge engines and their nacelles); that is than recovered improving the overall aerodynamics of the aircraft, with the introduction of winglets or increasing the wing surface. However, as per today, they arrived at a point where it is not possible to improve these engines anymore or getting important advantages from the ones of the competitors. Bypass ratios cannot be increased further, because of aerodynamical reasons, but also due to the fact that such big fans spin at very different velocities from the core to which are keyed, making necessary a gear to reduce the revolution per minute, thus introducing important and non-neglectable losses.

Furthermore, if we study the evolutive trends of aeronautical engines starting from 1960's up until today we noticed as seen in Figure 0.1, taken from reference [2], that we have arrived at a point where a new unseen engine typology is necessary in order to allow a further performance leap.

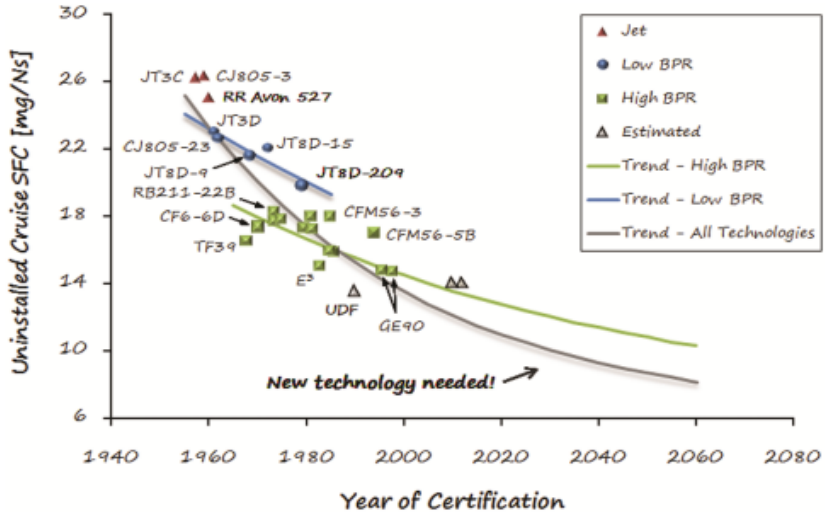

Figure 0.1: Evolution trends of aircraft engines

The ideas that can be found in publications, and that are currently studied from the main manufacturers are multiple and opposite to one another, bringing innovation from different parts. Everyone agrees on several points, that in the end are the ones dictated from airliners, whose demands are more and more stringent:

- Reduction of consumption and emissions
- Reduction of parts to be used
- Electrification of the aircraft

Those three needs are one a consequence of the other, and are defined at first from the higher and always increasing awareness of the population of the world for climate change, and the necessity to start thinking for a more sustainable future avoiding the use of fossil fuels. Despite the air traffic is responsible for less than 3% of the total of the greenhouse gasses emissions in the EU, amongst the sources of emissions that contributes to climate change, it is the one that grew faster. This phenomenon is caused, as said before, mainly by the record increase in the number of passengers, flights, and freight transportation around the world. This called for the governments to try to end this, introducing laws with the aim of reducing the emissions, thus forcing the manufacturers to look for a solution. An example of that is Denmark deciding to make all domestic flights fossil-free by 2030. [3] This has

brought the research, parallel to what has been done in the automotive sector, to move the investments on electric and batteries, as they seem the ideal solution, because they don't cause direct emissions. However, looking closely to this technology it can be seen that energy accumulators are not sufficiently advanced to be used profitably in a passenger plane, due to weights ad overall dimensions that will be discussed further on this thesis. Furthermore, productive volume and the way batteries are manufactured, are not as sustainable as it might appears: extraction of rare earths is done with the use of huge amounts of water (some estimates [4] talks about more than 50% of the local population water requirement), exploitation of workers, harmful gas emissions during the production, other than the fact that nowadays batteries are not recycled properly and in great amounts. Said that, it can be excluded that the main path for the evolution of aviation, for now, is to take the all-electric direction, if not for small aircrafts and drones with limited range.

Instead, it is important to look for an increasing electrification of the aircraft with electricity not only taken from batteries, but also generated from a thermal engine. The main producers already have done substantial changes in this way with the newer aircraft presented such as the Airbus A350-XWB and the Boeing B787 Dreamliner, where they went after a concept of More Electric Aircraft (MEA) where basically everything from entertainment systems to control surfaces, passing through avionics and safety devices, is powered by electricity produced with alternators placed in series with the engines. The only thing that stays purely mechanical is the thrust.

Now, seen all this pressure for greener aircrafts and for the commercialization of urban mobility vehicles to be versatile, so that with the same engine they could cruise but also take off and land vertically, engineers are studying ways to electrify the thrust too.

There is a simple answer to that, seen that there are electrical motors on the market with a weight to power ratio incomparable with the one of a modern turbofan. These motors are small and versatile, however they are not able to generate enough thrust to power a commercial plane. Therefore, multi-rotor configurations based on the concept of distributed propulsion are currently being developed. This is a new kind of propulsion system where the engines are distributed along the entire fuselage or the wings. This system could increase performance, propulsive and

overall efficiencies along with an improvement of aerodynamic effectiveness due to completely new shapes of the airframe and better integration of the propulsive system. An example of these ideas are the configurations studied by NASA such as the STARC-ABL, N3-X, or the ESAero eco-150 developed by a private competitor, where a series of small propellers embedded on the airframe are used to produce the thrust.

Figure 0.2: Example of distributed propulsion ESAero eco-150

The main problem remains how to produce the electric current necessary to operate these motors since batteries are too heavy for the purpose as per today.

The solution, maybe not the only one, but the one that will be developed in this thesis, is the utilization of a small thermal engine, precisely a gas turbine generator, with an alternator at the end, able to produce enough power to drive the electrical motors. The problem at this point is that those type of engines uses non renewable fossil fuels continuing to raise the pollutants emissions. This could be partially solved using alternative fuels derived from plants or waste products such as biofuels, massively reducing the small amounts of pollutant produced, and designing as well as possible every component in order to keep the emissions low.

The change of fuel could be also a great deal for airliners which in fuel have their biggest expense, seen that to this day, the prices of jet A-1 keep raising due to the geopolitical instability of the country responsible for its extraction and production. Thus, a new more efficient engine with renewable fuel would be well liked by the airliners.

Therefore, the main purpose of this thesis, will be to develop these ideas, starting from a small scale, thus designing a microturbine generator always working at its best efficiency, producing enough energy to fly a small light aircraft with an endurance of four to five hours and a range of about 1400 km similarly to the planes already available on the market. The main characteristics of this engine will be:

- Compactness and low weight

- Higher performance than an all-electric plane
- Use of different and sustainable fuels
- Consumption ad emissions comparable to the competitors
- Versatility to be adapted to other purposes

To do this, in the first place, the prototype plane upon which we will base our study will be presented, then different thermodynamic cycles will be addressed and analysed using the MATLAB software, introducing innovative components with the aim of compensating the weaknesses of basic gas turbines. One of the cycles will be chosen for our engine, and every component will be designed and developed using cutting edge materials in order to maximize performances.

1 Case study

To design our engine, we have to decide at which class of planes it will provide the thrust necessary. We wanted to design an engine with a power output between 100-500 kW therefore our choice fell on light aircrafts, UAV's and drones. After some research it has been decided to opt for a prototype developed by Airbus which flown for the first time in 2014: the Airbus E-fan. This plane is a two-seater, all-electric demonstrator with lithium-ion batteries powering 2 electric motors of about 30 kW each. Its autonomy is around 60 minutes. In Figure 1.1 is represented in all his shapes with main dimensions and characteristics.

Figure 1.1: Technical data E-fan 1.0

Seen that this is mainly a prototype that should have been upgraded to become a 4 seat plane and knowing that the objective for our engine was to produce a higher power than the one necessary for this plane to fly, it has been decided to rescale the dimensions of this aircraft with a ratio of 1:1.45. in this way we have a light aircraft that, at least theoretically, could compete in his sector with other planes such as the Piper PA-46 and the Cessna 210. Looking at these two aircraft cited here, and in order to become a valuable competitor, we want it to have a range of about 1400-1600 km or 4 to 5 hours of flight, and up to 5 seats. This because the

prototype built is clearly not suitable for air transport seen its autonomy around 1h and it can carry only two people.

To ensure this range of flight with only batteries, even using the best available on the market with a power density of 250 Wh/kg, in order to produce 100kW for 5 hours we would need about 2200 kg of batteries reaching a weight that is higher of the entire empty weight of the plane. This, even with a big improvement on battery energy density makes the full electric version of this plane not allowable. Therefore, the sector we intend to place our aircraft, an hybrid solution such as the one with the turbogenerator could be a worthwhile.

We present down here the main characteristic of our plane confronted with the other two.

Table 1.1:Main data of the prototype and confront with other planes

	E-Fan mod	**Piper PA-46**	**Cessna 210**
Wingspan [m]	13.78	13.11	11.20
Length [m]	9.67	8.6	8.59
Height [m]	2.9	3.44	2.95
Weight [kg]	1650	1969	1045
Lift to drag ratio [-]	14.1	/	10.9
Cruise speed [m/s]	80	109.7	99.4
Cruise height [m]	5000	Up to 9000	6100
Range [km]	1400	2487	1700
Engine power [kW]	100	260	230
Take off distance [m]	630	637	660
Landing distance [m]	/	600	460

2 Basic Brayton cycle

For our engine we decided to opt for a microturbine gas generator or “turbogenerator”. It is one of the simplest gas turbine engines and it is based as most of the airborne engine on a Brayton open cycle. This is a versatile thermodynamic cycle that can be used for massive ground installations for energy production as well as miniaturized engines that produces few watts of power. Without big modifications it can be used as a propulsive system for helicopters and propeller aircrafts, thus is the best candidate to be transformed in an energy output generator. Our cycle will be carefully modified to convoy all the surplus power generated from the combustion to the shaft and therefore to a generator that will convert it in electrical energy to power the electric motors behind the fans.

As a first thing, to see if this is a viable and convenient option, we will analyse the cycle in a general way, for different pressure ratios and determining the main parameters to have a whole idea of the engine strength and weaknesses.

To do so, we have developed a MATLAB code, as accurate as possible, that will help us studying the various configurations. In appendix A are reported all the characteristics of the code used and how we make it accurate, on most point of view.

In the next paragraphs the basic cycle will be addressed, some ideas for improvement will be suggested and from there we will start developing our engine.

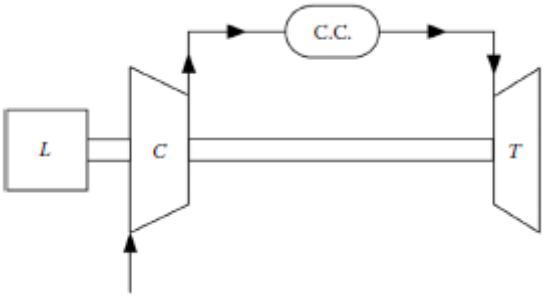

Figure 2.1: Basic cycle components [9]

2.1 Basic Microturbine generator

This type of cycle can be divided into three main steps that represent the key components of the engine (Figure 2.1):

- Compressor
- Combustion chamber

- Turbine

With other elements such as air intake and exhaust nozzle setting the fluid in the right state to be used, or the shaft and alternator whose job is to convoy the power generated and transforming it into electricity.

To better understand how this engine work, we can follow the journey the air does: starting from an undisturbed condition outside the engine, where the fluid has its own properties and a relative velocity that is the flight velocity, it enters in the engine by means of an air intake that slows it down preparing it for the entrance in the compressor. Here it undergoes a compression, up to the highest pressure point of the entire cycle, without big variations in speed, but with a strong increase in temperature. At this point the air is conveyed into the combustion chamber where it gets mixed with the fuel and burns. Here an exothermal chemical reaction happens, generating enormous amounts of heat and bringing the temperature to the maximum one of the entire cycle. The pressure drops a little due to head losses generated by friction in the chamber. The TIT (Turbine Inlet Temperature) is of extreme importance because it determines the performance of the cycle. Now the hot and pressurised gas is delivered to the turbine where it expands. The expansion makes the turbine rotate at high-speed carrying on the compressor and in our case the permanent magnet generator. The great addition of energy given by the combustion is therefore transformed firstly in rotational energy that drives the compressor and the remaining part goes into the generator and is then transformed. Finishing, the gasses with the remaining surplus of temperature, pressure and energy are delivered to an exhaust nozzle that discharges them into the atmosphere with a higher velocity, generating thrust. In our case most of the energy is taken out from the fluid by the turbine and transformed in rotational speed to be given to the generator therefore not a great amount energy remains for the nozzle to transform. The thrust generated is almost neglectable, as happens in rotorcraft, because it is generated elsewhere with electric motor-powered fans (or in case of rotorcraft by the rotor itself).

We can say that our engine is similar to a turboshaft/turboprop where instead of using the power generated to spin a shaft attached to a rotor or a propeller, we spin a shaft attached to an AC generator.

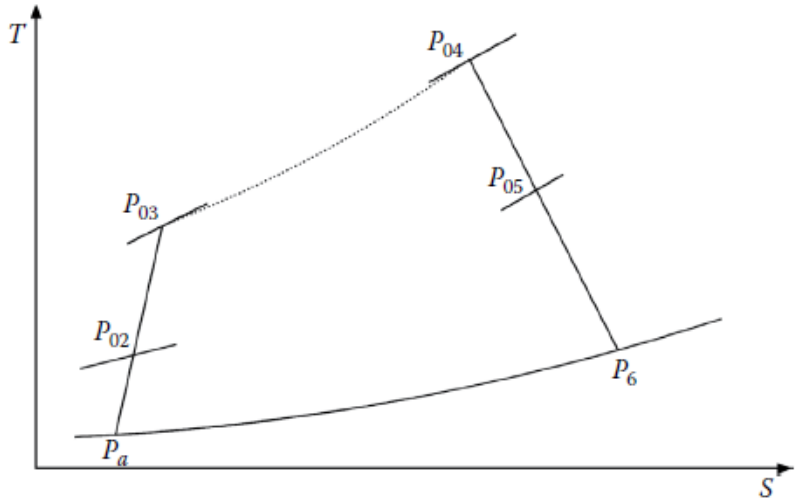

Figure 2.2: T-s diagram Brayton cycle

The temperature-entropy diagram reported in Figure 2.1 shows the real thermodynamic transformations that the fluid undergoes, accounting for irreversibility in the transformations of compression and expansion other than the pressure losses in the combustion chamber. The transformations happening cannot be considered reversible nor isentropic and efficiencies must be taken into account. This will bring important differences in the determination of the thermodynamical properties of the fluid at each station. Another big assumption we do is to assume that the fluid entering the engine is completely stopped, thus we can use the static quantities for the calculations. This is a huge simplification of the process but at the end it doesn't comport errors in the values determined.

2.2 Thermodynamics of the basic cycle

In this paragraph we analyse our base cycle from a thermodynamic point of view to better understand the variations of the two principal quantities: pressure and temperature.

First thing to do is to calculate the total temperature outside our engine, that will be equal to the temperature at the entrance of the engine because the transformation between undisturbed stage (a) and stage 1 can be considered isentropic, seen that no heat or work is exchanged. Thus:

$$T_{0a} = T_a + \frac{v^2}{2 \cdot Cp} \tag{2.1}$$

From now on when we talk about temperature and pressure in this paragraph, we refer to the total temperature and total pressure with the aim of simplifying our writing.

Entering the diffuser we have the first non-isentropic transformation, due to the non-reversibility of the losses caused by friction of the fluid on the walls. Pressure losses can be quantified introducing a diffuser efficiency as in equation (2.2). Therefor,e temperature and pressure after the diffuser section can be determined as:

$$\eta_d = \frac{T_{02\_is} - T_a}{T_{02} - T_a} \tag{2.2}$$

$$T_{02} = T_a \left(1 + \frac{k-1}{2} M_a^2\right) \tag{2.3}$$

$$P_{02} = P_a \left(1 + \eta_d \left(\frac{T_{02}}{T_a} - 1\right)\right)^{k/k-1} \tag{2.4}$$

We used an efficiency for the diffuser of 0.98.

Entering the compressor, the pressure raises up with an adiabatic non reversible transformation. We can see from the graph in Figure 2.3 that the pressure raise is important but not as big as it could be with an ideal transformation. Same thing can be said for the temperature increment. Those irreversibilities are determined with the isentropic efficiency of the compressor (2.5) that in turn are calculated as seen in appendix A from the polytropic efficiency whose value is taken to be 0.85. Other than this, having priorly decided the compression ratio,

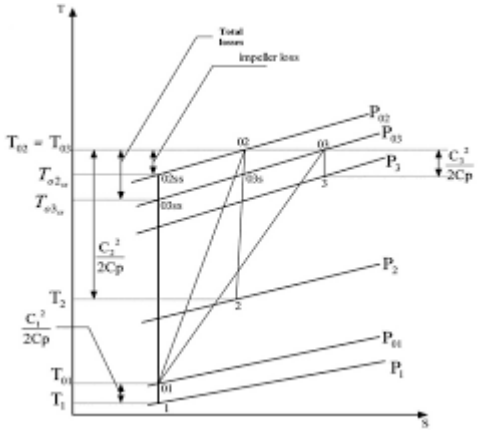

Figure 2.3:compression real vs ideal transformation

which is a project parameter ad will be determined after careful evaluations, pressure and temperature are determined as similarly done before.

$$\eta_c = \frac{T_{03\_is} - T_{02}}{T_{03} - T_{02}} \tag{2.5}$$

$$\frac{P_{03}}{P_{02}} = \pi_c \tag{2.6}$$

$$\frac{T_{03\_is}}{T_{02}} = \pi_c^{\frac{k-1}{k}} \tag{2.7}$$

The combustion process takes place between stages 3-4 and ideally has no pressure losses but the real transformation, always due to friction penalize the process. The combustion friction loss factor f_c is introduced (2.8) and a value of 0.98 is taken. At this point, since the TIT temperature T_{04} (that is also the maximum temperature at the exit of the combustion chamber) is a parameter to be decided based on the material of the turbine impeller, we can estimate from (2.9) the fuel to air ratio f that will give us the information on fuel consumption.

$$P_{04=} f_c \cdot P_{03} \tag{2.8}$$

$$(1 + f) \cdot Cp_h \cdot T_{04} - Cp \cdot T_{03} = f \cdot H_u \tag{2.9}$$

Looking at equation (2.9) we know the lower heating value H_u because it is a property of the fuel itself, and the specific heats of air and combustion gasses are determined through the equations described in Appendix A.

At this point gasses enter the turbine. Similarly to the compressor, the process is not reversible therefore an isentropic efficiency is in order to determine pressure and temperature at the exit of the stage. The gasses are convoyed to the nozzle where total temperature and pressures remains equal, but the temperature varies due to the efficiency of the nozzle. Knowing that the last piece of enthalpy drop is transformed entirely into speed/trust, the nozzle exit speed can be derived:

$$\eta_{ozzle} = \frac{T_5 - T_6}{T_{05} - T_{6\_is}} \tag{2.10}$$

$$V_{discharge} = \sqrt{2 \cdot Cp_h \cdot (T_{05} - T_6)} \tag{2.11}$$

We need to make sure that the discharge pressure is the ambient pressure so that we can consider the nozzle adapted.

2.3 Characteristic parameters of the engine

There are various performance parameters that are used to determine the overall goodness of an engine: specific power (SP), specific thrust, specific fuel consumption (SFC) and efficiencies.

The specific power is the net power generated by the turbine excluding the power used to spin the compressor. Therefore, it is the power used to generate the thrust, and can be calculated as such:

$$\mathrm{SP} = \frac{\mathrm{P_n}}{\dot{\mathrm{m}}} \tag{2.12}$$

The specific thrust is determined adding to the thrust generated by the fans the contribute given by the exhaust nozzle, all divided by the mass flow rate.

$$\frac{\mathrm{T_{tot}}}{\dot{\mathrm{m}}} = \frac{\mathrm{T_{nozzle}} + \mathrm{T_{fan}}}{\dot{\mathrm{m}}} \tag{2.13}$$

$$\mathrm{T_{nozzle}} = \dot{\mathrm{m}} \cdot \left(\mathrm{V_{discharge}} - \mathrm{v}\right), \quad \mathrm{T_{fan}} = \dot{\mathrm{m}}_{\mathrm{fan}} \cdot \left(\mathrm{V_{post\_fan}} - \mathrm{v}\right) \tag{2.14}$$

One great parameter to understand the performance of our engine is the specific fuel consumption, that is the ratio between the fuel flow rate and the net power generate by the engine.

$$SFC = \frac{\dot{\mathrm{m}}_{\mathrm{fuel}}}{\mathrm{P_n}} \tag{2.15}$$

Efficiencies give an overall perspective of the engine summing up the other parameters and allowing for a performance confront with other types of motors. In equations (2.16-2.18) are written respectively the expression for: thermal, propulsive and total efficiencies.

$$\eta_t = \frac{P_n}{P_{chemical}} = \frac{P_n}{f \cdot \dot{m} \cdot H_u} \tag{2.16}$$

$$\eta_p = \frac{T_{tot} \cdot v}{P_{getto}} \tag{2.17}$$

$$\eta_o = \eta_t \cdot \eta_p \tag{2.18}$$

Knowing how the basic engine work and how to determine the thermodynamical characteristics at every step we can now analyse thoroughly our engine.

2.4 Normal turbine generator evaluation

To determine the fundamental parameters, we have to define some project values. Since we are only interested in specific parameters and efficiencies, we will define randomly the mass flow rate entering the engine. Other two parameters such as compressor pressure ratio and TiT will be taken variable to better analyse the engine in different situations. In particular, three values of temperature are taken (1403 K – 1503 K – 1603 K), and a range of π_c from 0 up to 50. Flight speed and cruise altitude are respectively 78.3 m/s and 5000m.

Another thing to be defined is the division of the enthalpic drop between turbine and exhaust nozzle. Since we want the biggest part of the thrust to be generated from fans the majority of the ΔH will be done in the turbine leaving to the nozzle only a small portion useful to accelerate the flow at speeds slightly higher than the cruise one. After having analysed thrust variation in function of the percentage of enthalpy drop in the nozzle as can be seen in Figure 2.4Figure 2.5, we can conclude that in order to maximize the total thrust generated by our engine the ΔH should be of the order of 1%. For our case we will use 0.6%.

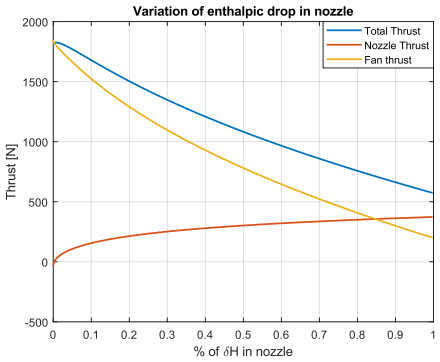

Figure 2.4: variation of thrust with percentage of entalpic drop in nozzle

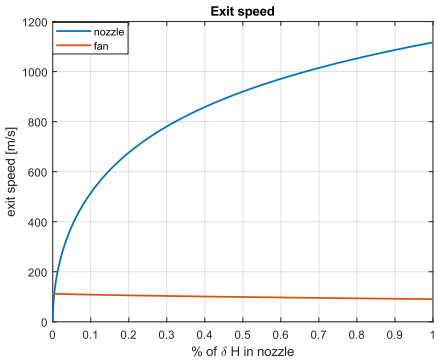

Figure 2.5:variation of exhaust speed with percentage of entalpic drop in nozzle

2.4.1 Results obtained

Having done all the premises, we now proceed running our code and examining the results we get.

Starting with the specific power in Figure 2.6 we see the trend of the curve in function of pressure ratio (pr) and temperature. Power has a maximum between pr of 10 to 20 that moves to the right with the maximum cycle temperature. This is because the higher the TIT the bigger the enthalpic drop in the turbine for the same power requested from the compressor. The specific fuel consumption behaves in an opposite way with decreasing values for increasing pr. This can be explained saying that with an higher pressure ratio higher temperature values are reached before the combustion chamber, thus less fuel is needed to arrive at the maximum temperature.

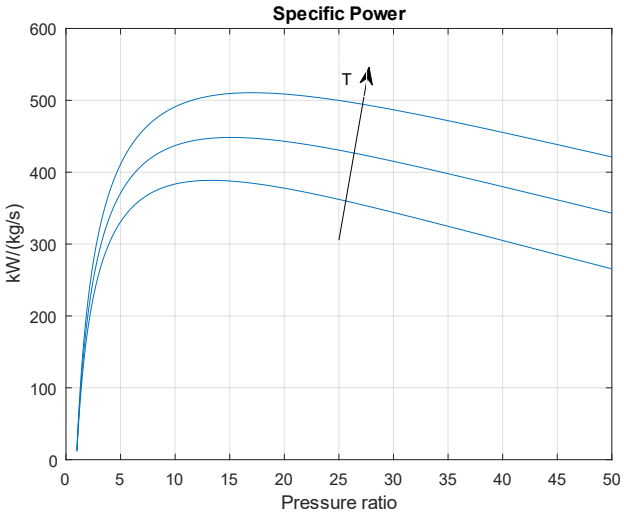

Figure 2.6: Specific power in function of temperature and Pr

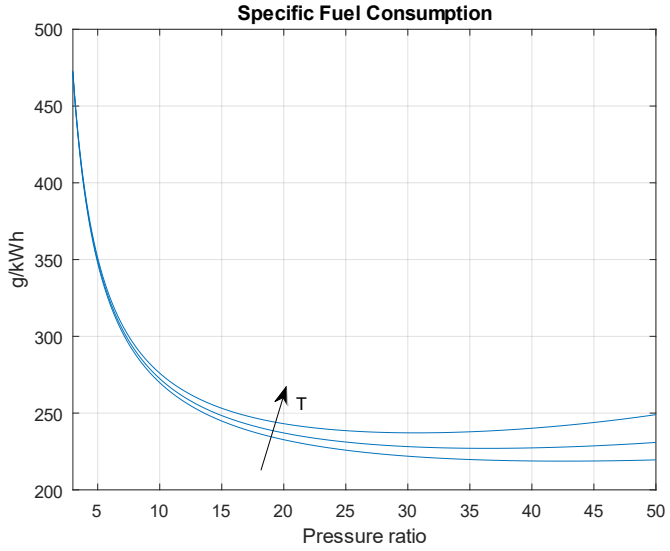

Figure 2.7: Specific fuel consumption in function of temperature and Pr

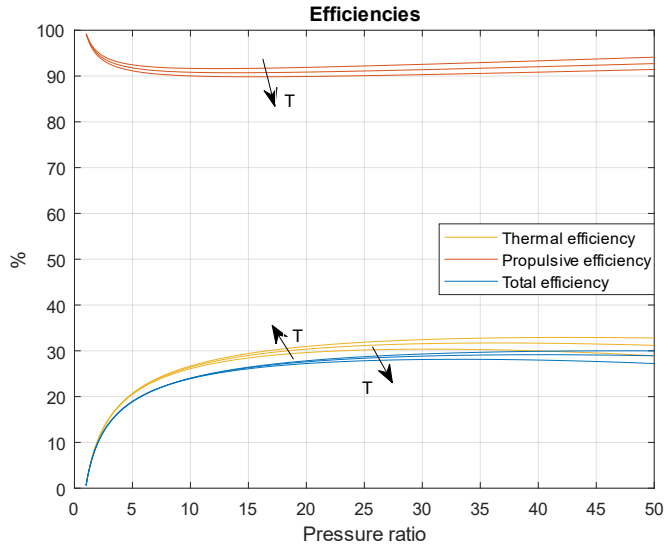

Figure 2.8: Efficiencies in function of temperature and Pr

The efficiencies present extremely different values to one another. The thermal one tends to grow with the pressure ratio and increases his value with higher maximum temperature. This value gives an idea of how well the energy introduced with the combustion is transformed into propulsive energy, the higher the value the better the cycle works. It never reaches high numbers due to the losses of the engine, but it is important when designing to take it at is highest values. Propulsive efficiency has extremely high percentages that remains more or less constant in our case, a part for pr up to 5 where we have a minimum. When the maximum temperature increases the propulsive efficiency decreases because even the discharge

temperature and velocity rise making thrust power (P_{getto}) higher and consequently the efficiency smaller. The total efficiency follows a similar path regarding the temperature, with an increasing value with the pressure ratio. This efficiency always stays at low values and usually does not exceed 30%.

2.5 Final considerations on basic cycle

From these graphs we can draw some considerations and find a path for a correct and intelligent development of our microturbine gas generator. Since we want to build an engine that is as fuel efficient as possible the TIT temperature must be higher than normal but within the limits of the material currently available, so at a first glance 1503 K could be a correct hypothesis for our engine. The values of the efficiencies are not super high as we want them to be especially in the low range of pressure ratios usually used in microturbines. The only parameter that doesn't seem to be a problem is the specific power that looks to be high enough to produce the power we need. Therefore, there is a need to find solutions to improve efficiencies especially the thermal one, fuel consumption and in general to shift the maximum of the curves (minimum for SFC) further to the left in order to have them to an acceptable pressure ratio value, allowing for small turbomachines and an overall engine dimension.

These solutions will be discussed and developed in the next chapter.

3 Intercooler & Recuperator

Having seen characteristics and problems of the basic gas turbine generator we now try to implement some solutions to achieve better results suitable for our application, remembering that the engine must be of feasible dimensions and possibly weight less or similar to the weight of the batteries of the initial prototype. To do so, after analysing various solution available in literature, even for gas turbines for ground or maritime operation, it has been decided to opt for two heat exchangers:

- Intercooler
- Recuperator

They are usually not used in commercial jet engines because of their massive dimensions and weight for the gain they provide, but the first is often used in automotive application and the second one is a fundamental part of all turbines for electricity generation to the ground, or where dimensions are not a concern. They apparently work in opposite “direction” since one is used to cool the flow down and the other to heat it up, but used in the right place, they both provide huge benefits. Both of them will be studied singularly in a cycle to better understand their qualities and defects. Then they will be used together, and a confrontation will be done to decide which setup is the best one to be used for our application.

3.1 Intercooler

An intercooler is an air-to-air heat exchanger that uses a cold flow usually taken from the outside air to cool the gas down after the first stage of compression before entering the second stage. In this way we obtain a colder and denser fluid entering the second compressor. As understandable, to use this element we need to split the compressor in two stages if axial or into two compressors if radial ones. This will allow for smaller diameter dimensions for the same pressure ratio, or higher pressure ratios with the same diameter. Using this heat exchanger, the second compressor needs less power to work, therefore a higher power is available for the generator to be transformed into electricity. Specific power improves with the efficiencies remaining almost unchanged, at the expense of the specific fuel consumption that increases. This because the temperature at the exit of the compressor in

respect with a normal cycle is lower causing a greater need of fuel to allow the gasses to reach the maximum temperature in the combustion.

It may look like using this device could go against our need have to the lowest fuel consumption possible, and even if dimensions gets smaller, adding a new element contributes to increase the weight. We will see though that this exchanger could be a valuable option in some cases and conditions.

Geometry, dimensions weight and overall performance of this device will be discussed further in chapter 8.

Graph presented in this chapter are all plotted in the same conditions with same output power and thrust.

3.1.1 Performance analysis of intercooler setup

Introducing an intercooler into our engine and therefore adding it to our MATLAB code, will require as said splitting the compressor in half. To have a determined pressure ratio the pr of the first stage multiplied to the pr of the second stage has to return the ratio we want. This is done having each turbomachine to compress the air of the square root of the total pressure ratio (3.1) in this way we manage to have two balanced compressors requesting a similar amount of work.

$$\pi_{c\_1} = \pi_{c\_2} = \sqrt{\pi_{c\_tot}} \tag{3.1}$$

The air exiting the first compressor enters into the intercooler where it is cooled down by an airflow coming from a second air intake and having a temperature equal to the one of the outside atmosphere. The two fluids exchange heat for convection with crossflow paths to maximize the exchange.

The maximum amount of heat passed from the hot fluid to the cold one is calculated using equation 3.2. The maximum heat to be exchanged is function of the temperature of both fluids and C_{min} is the minimum product of the mass flow rate and specific heat of one of the fluids. The effectiveness of the intercooler plays an extremely important role in determining the performance of this device and allows us to calculate the exit temperature of the flow. Usually extremely high efficiencies can’t be achieved by this device in constrained spaces due to the elevated quantity

of cold flow that has to be brought inside. Values over 90% are unattainable, but with a good design an efficiency in the range between 40%-80% is achievable.

$$q_{max} = C_{min}\left(T_{03\_c1} - T_a\right) \quad where\ C_{min} = min[\dot{m} \cdot Cp] \tag{3.2}$$

$$\varepsilon_{ic} = \frac{T_{post\_ic} - T_{03\_c1}}{T_{03\_c1} - T_a} \tag{3.3}$$

Another important thing to be taken into account is the pressure drop due to friction of the fluid on the walls of the intercooler. It must be as small as possible in order to avoid performance degradation and to jeopardize the work done in the compressors. Seen the basic of this element we find useful to plot the performance parameters of the engine in function, not only of pressure ratio, but also of the effectiveness of the intercooler in a range from 0 to 100%.

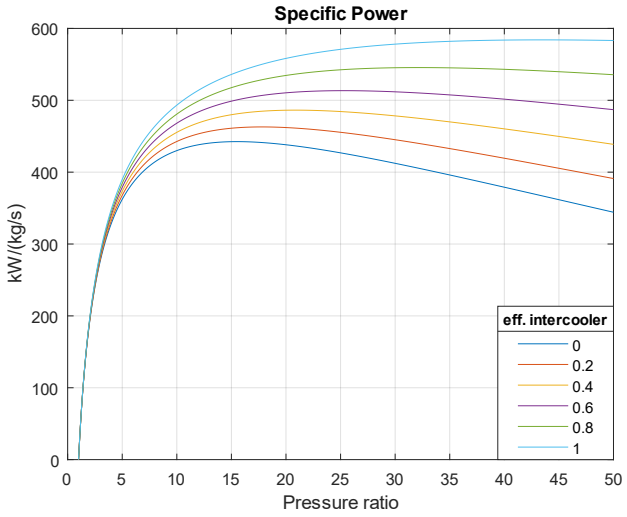

Figure 3.1: Specific power in function of Pr

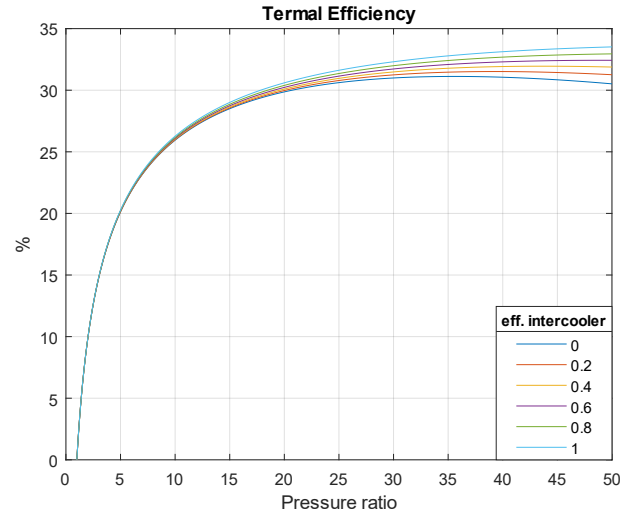

Figure 3.2: Thermal efficiency in function of Pr

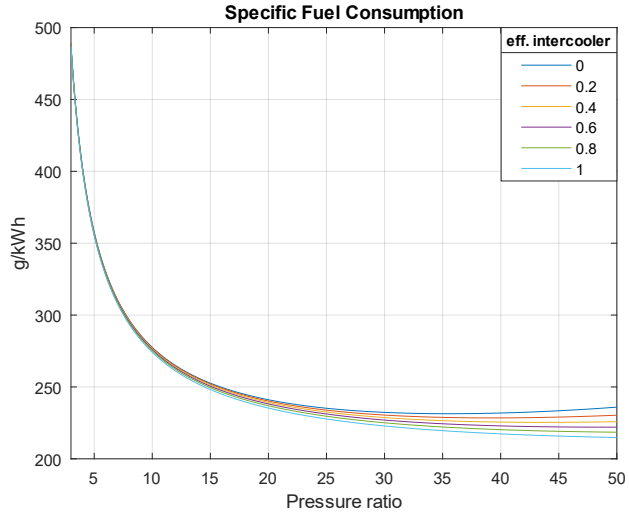

Figure 3.3: Specific fuel consumption in function of Pr

We can notice how values of Specific power and thermal efficiency are higher than the ones seen in chapter one for the normal gas turbine generator, and we have as expected a small increase in fuel consumption that reduces with higher intercooler efficiencies. About effectiveness we see that they play a massive role in increasing power and thermal efficiency of the engine mostly at high pressure ratios, with contained effect at smaller ones. Peak values for every graph tend to move further right with the efficiency due to the fact that the two installed compressors require less work to rotate providing a higher net power generated to be delivered to the generator.

After this small evaluation of the results obtained, we can confidently say that this configuration seems promising only if we can reach values of pressure ratio above 15 and intercooler effectiveness as high as possible to mitigate the effect on fuel consumption.

3.2 Recuperator

A recuperator is an air-to air or gas-to-air heat exchanger used in basically every ground application gas turbine for the generation of electricity. It is based on the fact that after the turbine, the fluid heading into the exhaust nozzle and then into the atmosphere has still an extremely high temperature. This property is even more important in microturbines where the turbine doesn't expand much leaving the fluid at an even higher temperature. The hot gas instead of being directly expelled, passes through this heat exchanger placed between the compressor and the combustion chamber, heating the air before it enters the combustor. This allows to avoid the enthalpic and thermic jump to be done entirely by the fuel thus saving a great amount of fuel without compromising the power output, but slightly reducing the thrust produced by the nozzle. Ideally the airflow could enter the combustion chamber at the temperature of the exhaust gasses, but in reality, the efficiency of the recuperator can't be 100% because we would need an infinite exchange area. These devices are effective even at small efficiencies, but in order to be convenient for aeronautical application they have to have extremely high efficiency >90% and low-pressure losses due to friction or other impediments, lower than 5%. This makes it difficult to have it at a low cost, low weight and small dimensions, and it is one of the main reasons it is still not used in commercial engines.
The design, dimensioning and material selection will be done further in this thesis at chapter 8.

3.2.1 Performance analysis of recuperator setup

To develop our setup in MATLAB, equations similar to the ones for the intercooler will be used, this time with a singular compressor and turbine, rearranging a little bit the initial code developed. The heat exchanger is developed as a counter flow system with a big exchange area to maximize the effectiveness.

$$q_{exchanged} = \varepsilon_{rc} \cdot q_{max} \quad where \;\; q_{max} = C_{min}(T_{05} - T_{03}) \tag{3.4}$$

$$\varepsilon_{rc} = \frac{T_{post\_rc} - T_{03}}{T_{03} - T_{05}} \tag{3.5}$$

Where T_{post_rc} is the temperature at the exit of the recuperator, T_{03}, T_{05} are respectively the one at the outlet of the compressor and the one exiting the turbine. Pressure drop is taken to be 4% and the effectiveness variable between 50% and 90% in order to understand how our engine behaves in different conditions. As before we plot the performance parameters in function of pressure ratio to have the same judgement parameters.

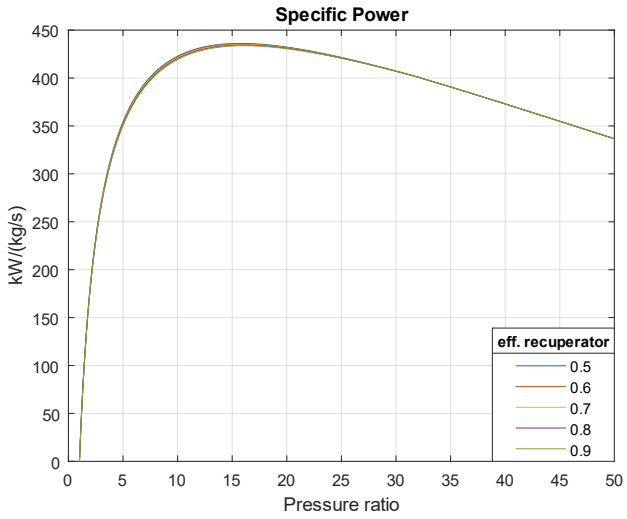

Figure 3.4:Specific power in function of Pr

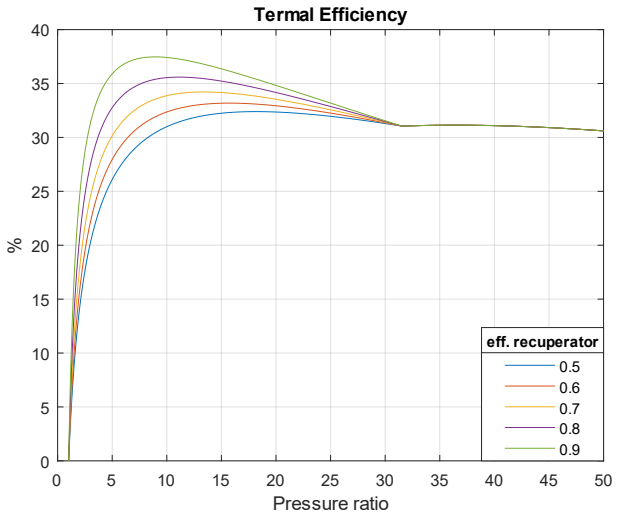

Figure 3.5:Thermal efficiency in function of Pr

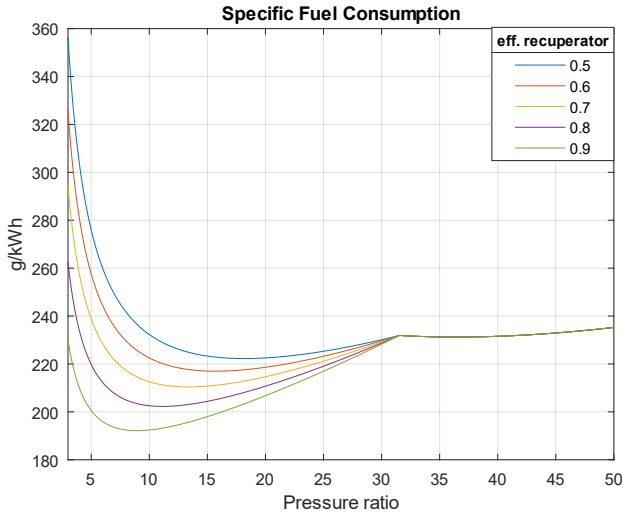

Figure 3.6: Specific fuel consumption in function of Pr

The results obtained are congruent with the one expected, and the ones available in literature. The specific power doesn't change significantly with the effectiveness of the exchanger and is attested at values similar to the ones seen in chapter 2 for the basic gas turbine. Fuel consumption and thermal efficiency report great improvements, with the first reaching values up to 20-30% lower than the intercooled version, and the latter having values over 35% at small pressure ratios, and overall excellent numbers. In the last two graphs it is clearly visible a point where all the efficiency curves converge, continuing as a unique one. This is the situation where because of the high expansion ratio, the turbine reaches a point where the temperature of the gasses at its exit is equal or smaller to the temperature of the air after the compressor. Therefore, after this point, the recuperator is not convenient anymore, but it is also counterproductive because the heat is transferred in the opposite direction, lowering the temperature at the entrance of the combustor. After this point that is at about π_c=31 this configuration will not be considered. Another interesting thing that can be caught from the graphs is the tendency of the curve's maximum (minimum for SFC) to shift to the left as the efficiency of the recuperator gets higher. This is optimal for our application that request small dimensions and consequently low-pressure ratios to be considered a good alternative to current engines.

Surely this option is a valuable one and will be taken into consideration for our purposes, even with small or low-efficiency recuperators.

3.3 Intercooler and recuperator setup

Seen that both configurations work extremely well if used with the right pressure ratios and efficiencies it has been thought to use the two heat exchangers together to see if the strength of each configuration could be maintained and the weaknesses eliminated or reduced to acceptable values. In particular, the smaller power available on the recuperator configuration could be balanced with the help of the intercooler and the high fuel consumption of this last element improved by the use of a regenerator.

The configuration consists in two compressors, a low-pressure stage and an high pressure one, divided by an intercooler, a recuperator, a combustion chamber and two turbine stages with the last one directing the gas to the recuperator before expelling it through the nozzle.

To plot the graph as done in the previous paragraph for other setups we restrict the range of the efficiencies of the two heat exchangers:

- *Intercooler* 40%-60%-80% which are the most plausible to use
- *Recuperator* 50%-70%-90% because in literature some exchanger with these efficiencies have been found

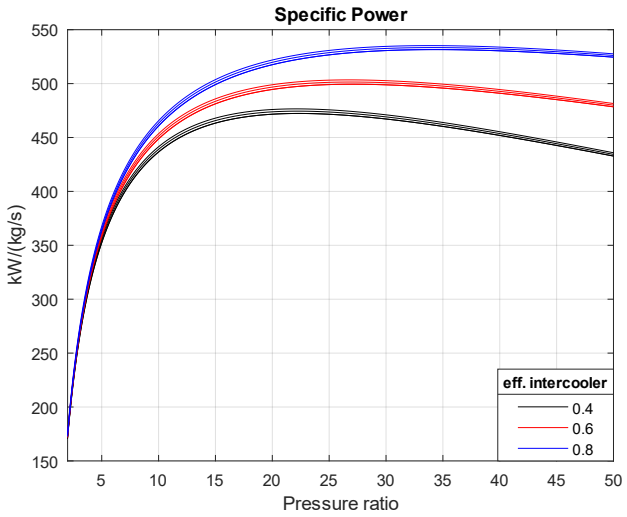

Figure 3.7: Specific power in function of Pr

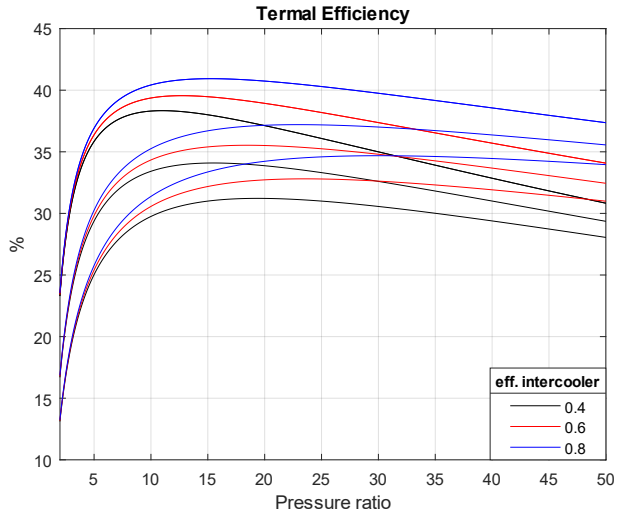

Figure 3.8: Thermal efficiency in function of Pr

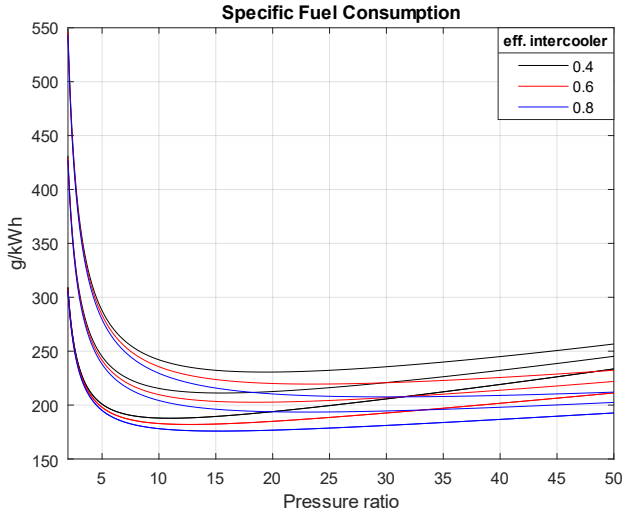

Figure 3.9: Specific fuel consumption in function of Pr

For a better understanding of the graphs the curves generated are grouped in colours by the efficiency of the intercooler. Curves with the same colour have a different recuperator efficiency and they vary as done in the previous chapter for the recuperator configuration, hence with a higher effectiveness of the exchanger, specific power and thermal efficiency get higher values instead for the specific fuel consumption we obtain lower values.

As expected, the results found are very promising and they mix both the configurations developed before. Specific power shows value similar to the intercooler-only setup, and the SFC reaches values well below 200 g/kWh for certain pressure ratios, an important improvement over the other configurations, as well as for the values

of thermal efficiency that are unseen in a jet engine and in general in an aviation engine. It is also important to see that the best parameters are in the range of the low-pressure ratios and never higher than 30.

In order to better understand this configuration, we must decide which effectiveness value assign to each heat exchanger. after having consulted other project and exchangers developed (more about that at chapter 8) and found in literature we came to the conclusion that for the intercooler, in an effort to maintain it small we chose a value of 60%. for the recuperator instead basing on the experience of capstone microturbines we are confident we can reach a 90% effectiveness in small spaces and with low density materials.

We plot then the curves obtained with this configuration.

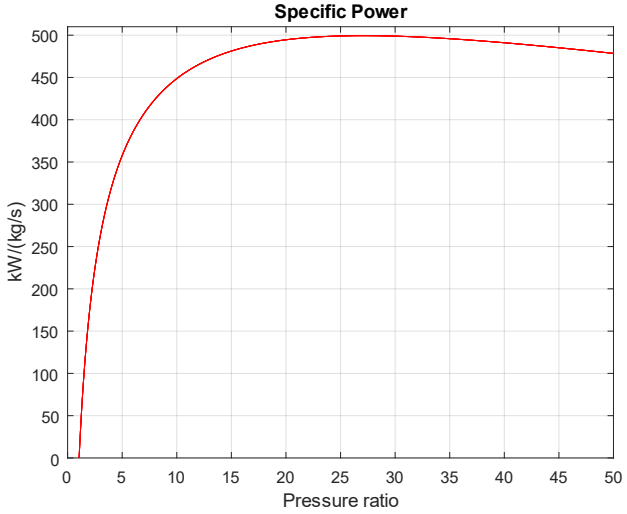

Figure 3.10: Specific power in function of Pr

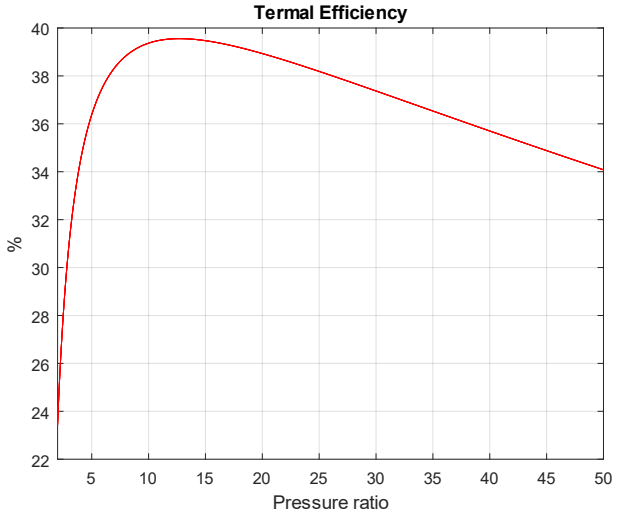

Figure 3.11: Thermal efficiency in function of Pr

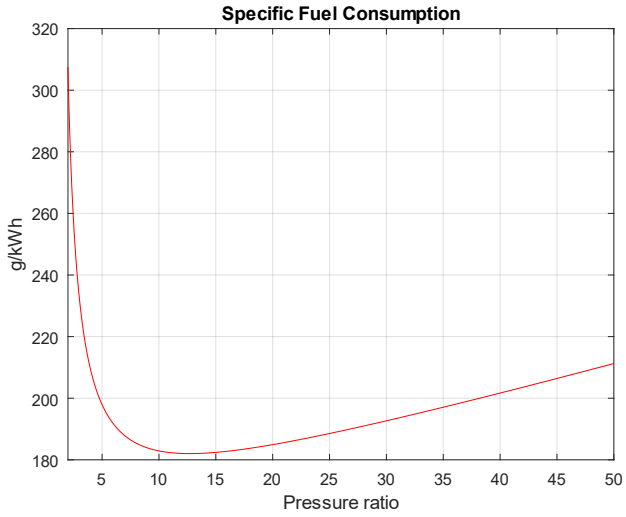

Figure 3.12: Specific fuel consumption in function of Pr

From these graphs we can clearly see that this setup expresses the best performance at pr values between 10 and 20 dependently to which graph we use and to which parameter we value the most.

But this configuration pays the fact that has two heavy heat exchangers and 4 pieces of turbomachinery that could make it not too convenient for our purposes eve if it is without any doubt the most efficient one. Before making the choice, a numerical confrontation is to be done with fixed pressure ratios between the three configurations involving also weights. In this way we can correctly choose the best setup and proceed with the design of the components.

3.4 Numerical comparison

To have an accurate comparison we chose to confront the different setups initially with the same pressure ratio, set to be 5, because it is a value usually not passed by microturbines, and consent to have small turbomachines of centrifugal type, contrarily to the use of high compression values where we must look into axial compressors or at least two different centrifugal ones. On the other hand, we choose to see the real potential of each configuration using different pressure ratios near the optimum point. Results are presented in Table 3.1and Table 3.2. From the first one we can see a clear reduction of consumption with the introduction of the recuperator in terms of kg of fuel per hour, and a reduction of mass flow entering the engine with the intercooler, thanks to the smaller compressors requiring less air entering. But with such a low-pressure ratio, substantial differences are not

appreciable, especially when the intercooler is introduced that looks almost useless in this case. As a matter of fact, if we look at the last two engines there aren't vantages introducing the second heat exchanger, the fuel consumption is even higher, so that it could be convenient not to use it in order to save on overall weight and size. But in this case neither of the configurations work at its optimal point so that the true potentiality of these engines is not noticeable here, but looking at Table 3.2 important differences can be detected. Since we are looking to minimize fuel consumption, we took the optimal pressure ratio for the SFC parameter. The results are always compared assuring that all the three engines deliver the same net power to the generator. From the data we notice that thermal efficiency increases with the complexity of the setup, the fuel expenditure undergoes a massive reduction, and the introduction of the intercooler allows for an important decrease in mass flow. Seen the whole picture, even if the two-exchangers setup seems to be the most performing, we are not sure that a fuel saving of about 2kg/h and a reduction in mass flow (that means a reduction also in the dimensions of heat exchangers) justifies the introduction of the intercooler. Therefore, a whole analysis on weights, taking into account their variation with the entering mass flow rate, is fundamental to make the most accurate decision. At this point we feel that the intercooler-only setup could be discarded seen that most of the parameters studied are inconveniently higher than the other designs.

Table 3.1:comparison between the three setups with Pr=5

	Normal	***Intercooler***	***Recuperator***	***Intercooler + Recuperator***
Cruise altitude [m]	5000	5000	5000	5000
Flight speed [m/s]	78.415	78.4	78.38	78.4
Pressure ratio []	5	5	5	5
Heat exchangers efficiency []	/	0.6	0.9	***Ic:*** 0.9 ***Rc***:0.6
Available Power (P_{getto}) [kW]	100.02	100.04	100.02	100.01
Net Power produced by turbine [kW]	128.577	128.714	128.608	128.402
Total thrust [N]	1146.99	1147.226	1147.366	1147.337
Thermal efficiency [%]	20.62	20.20	35.90	37.57
Mass flow rate [Kg/s]	0.3466	0.3397	0.3671	0.3328
Inlet Area [m^2]	0.006	0.0059	0.0064	0.0058
Inlet diameter [cm]	8.74	8.66	9.00	8.57
Fuel weight for one hour flight [kg]	44.893	45.878	25.791	24.607

Table 3.2:comparison between the three setups with Pr optimized

	Intercooler	***Recuperator***	***Intercooler + Recuperator***
Cruise altitude [m]	5000	5000	5000
Flight speed [m/s]	78.6	78.4	78.4
Pressure ratio []	16	8	14
Heat exchangers efficiency []	0.6	0.9	***Ic:*** 0.6 ***Rc***:0.9
Available Power (P_{getto}) [kW]	99.99	100.01	100.00
Net Power produced by turbine [kW]	126.81	126.79	126.845
Total thrust [N]	1147.137	1147.33	1147.20
Thermal efficiency [%]	29.23	37.21	39.32
Mass flow rate [Kg/s]	0.2429	0.2982	0.2690
Inlet Area [m^2]	0.0042	0.0047	0.0047
Inlet diameter [cm]	7.31	7.71	7.70
Fuel weight for one hour flight [kg]	31.234	25.07	23.92

3.5 Weights and final comparison

It has been decided to introduce a comparison with weights to have an overall glance, seen that as per now there is not a clear winner between different types of engines. Therefore, in this paragraph weights efficiencies and fuel consumption varying with pressure ratio and effectiveness of intercooler and recuperator are analysed. We do not consider specific power because we have already understood that those engine are easily able to produce the power we need. The intercooler-only setup has been excluded due to the elevated consumption (>30kg for 5 hours of flight).

As basic parameter a core engine weight of 30 kg has been taken, comprising compressors, shaft, turbines and combustion chamber. The fuel is determined with varying pressure ratio, for a flight time of five hours. We use for the calculation cryogenic liquid Methane (LNG) at -162°C because is denser than the normal one and therefore can be stocked in less space. This brings us to the weight of the tank. Initially we made the hypothesis of 10% the weight of the fuel inside, but having found an American company producing them in composite for aerospace applications [] and examining their numerous fuel tanks we derived a linear equation (3.6) to determine the weight of the fuel in function of the litres of methane needed, in this way seen that composite can be modelled in various forms and adapted to our necessity we can use a correct size tank instead of the ones sold on the market.

$$Tank\_weight[kg]=0.0695*liters\_of\_Methane +0.1648 \tag{3.6}$$

Regarding the weight of the heat exchangers, we refer to chapter 8 where a proper dimensioning of the elements is done and explained. We cand say that it is done calculating the exchange area with the ε-NTU method and compared with existing ones to see if we were getting similar results. For the intercooler aluminium was used, instead silicon nitride for the recuperator.

Integrating this assumption in the MATLAB code we were able to plot the weights in function of pressure ratio and effectiveness. Starting with:

- ***Recuperator-only configuration***

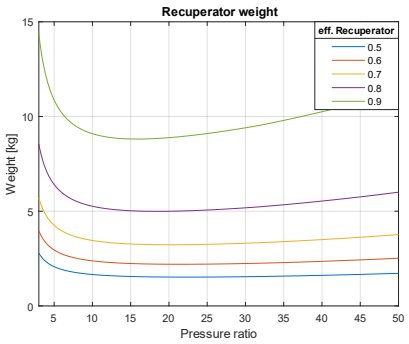

Figure 3.13 Recuperator weight in function of Pr

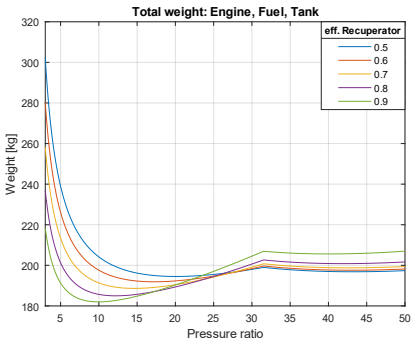

Figure 3.14: Total weight in function of Pr

It can be noticed how the total weight is around 180-200kg for optimal pressure ratio between 10 to 15. As noticable the recuperator gets heavier with pressure ratio and effectiveness. It needs to be remembered that if we want a single centrifugal compressor for this setup we must stay inside a pr of 5 because the ones available on the market do not get higher than this. We report in the following table the main variables for a pr of 5.

Table 3.3: Values of weight and efficiencies rec. only setup

Parameters	***Values***
Core weight [kg]	30
Fuel weight [kg]	128.93
Tank weight [kg]	21.50
Recuperator weight [kg]	10.87
total weight [kg]	191.30
Recuperator exchange Area [m^2]	14.31
Pressure ratio [-]	5
Recuperator Efficiency [-]	0.90
Thermal Efficiency [%]	35.90
Propulsive Efficiency [%]	89.89
Total Efficiency [%]	32.28

- ***Intercooler & Recuperator configuration***

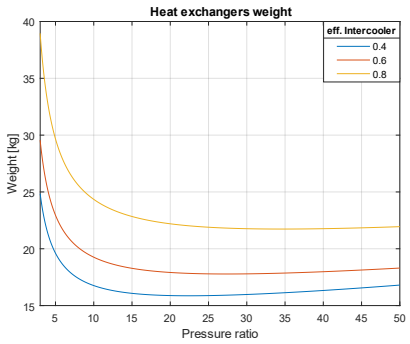

Figure 3.15: weight of heat exchangers in function of Pr

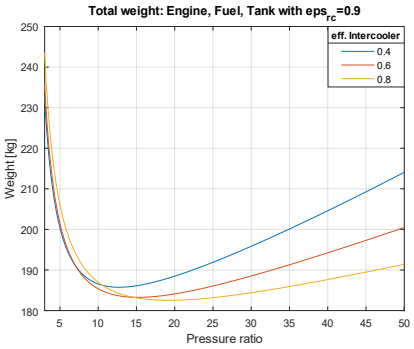

Figure 3.16: total weight in function of Pr

We chose to plot the curves only in function of the intercooler effectiveness thaking the one of the recuperator to be 0.9.

In this case in can be noticed that the minimum are for pr between 12 and 20 with vaues well under 190 kg for the total weight. In order to avoid a big intercooler its efficiency will be taken to be 60% so the red curve is the one to watch. We report in Table 3.4 the main parameters for this configuration with an optimal pressure ratio of 15.2 (divided in two compressors of 3.9 each).

Table 3.4: Values of weight and efficiencies 2 exchangers setup

Parameters	***Value***
Core weight [kg]	30
Fuel weight [kg]	115.69
Tank weight [kg]	19.31
Recuperator weight [kg]	7.87
Intercooler weight [kg]	10.25
total weight [kg]	183.13
Recuperator exchange Area [m^2]	10.94
Intercooler exchange Area [m^2]	1.95
Pressure ratio [-]	15.2 (2x 3.9)
Recuperator Efficiency [-]	0.90
Intercooler Efficiency [-]	0.60
Thermal Efficiency [%]	39.46
Propulsive Efficiency [%]	90.21
Total Efficiency [%]	35.60

With the two tables in mind and all the confrontations done in the previous paragraph , it's clear that the two heat exchangers configuration is the right one for our aircraft thanks to a smaller overall weight, lower fuel consumption (13kg less in 5 hours), and teoretically amazing efficiencies with the thermal one that almost touches the 40%, and the total greater than 35% unseen for an aircraft engines. Thanks to this amazing parameters the additon of the intercooler is a feasible choice to make.

At this weights needs to be added the electric current generator and the buffer batteries for other 20/30 kg, moving the total up to 200/210kg, well under the 2 tonns needed to fly using only batteries, and even under the weight of the current batteries used in the prototipe plane (220kg) that makes it fly for 1h.

3.6 Thermodynamical properties and other parameters of the cycle

In this paragraph are reported at each step the thermodynamical properties of the cycle chosen and other useful parameters used for the design of the components.

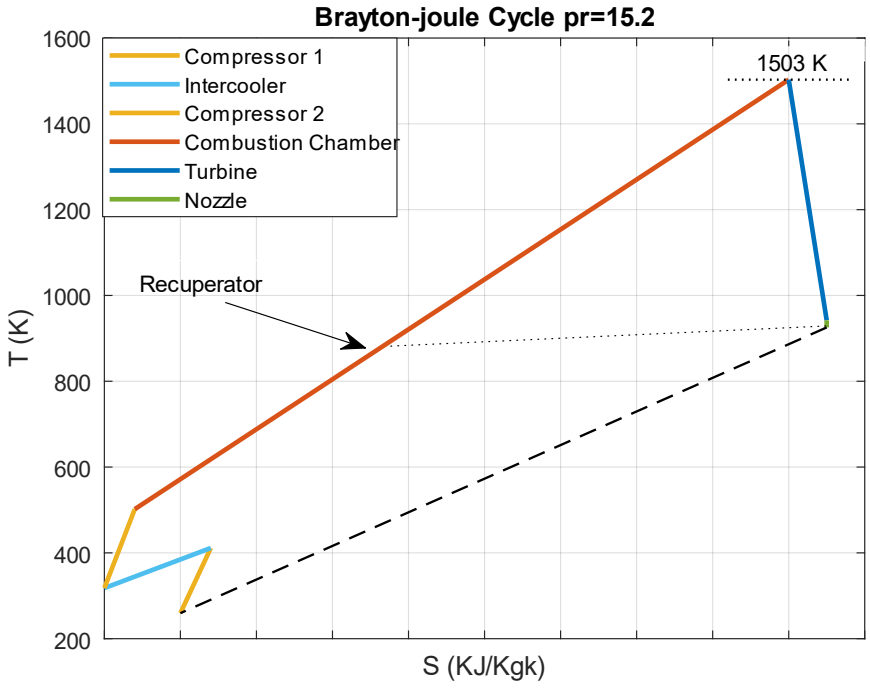

Figure 3.17: T-s diagram of final setup

<table>
<tr><td colspan="2"><u>FLIGHT PARAMETERS</u>:
Flight altitude 5000m
Atmosphere temperature T_a= 259.47 K
Atmosphere pressure P_a= 54014 Pa
Air Density 0.7362 kg/m^3
Cruise speed V_{cruise}=78.6 m/s
Mass flow rate $\dot{m} = 0.2631$ kg/s</td></tr>
<tr><td><u>02-DIFFUSER:</u>
Efficiency η_d=0.98
Exit temperature T_{02}=254.47 K
Exit pressure P_{02} = 56812 Pa</td><td><u>03-COMPRESSOR 1</u>
Polytropic efficiency η_{pol}=0.85
Isentropic efficiency η_{c1}=0.8194
Pressure ratio $\pi_c = 3.9$
Exit temperature T_{03}= 411.35 K
Exit pressure P_{03} = 221500 Pa
Power requested P_{c1}=39.84 kW</td></tr>
<tr><td><u>INTERCOOLER</u>
Effectiveness η_d=0.98
Pressure drop =3%
Exit temperature T_{03_ic}= 317.93 K
Exit pressure P_{03_ic}=214860 Pa</td><td><u>03_C2-COMPRESSOR 2</u>
Polytropic efficiency η_{pol}=0.85
Isentropic efficiency η_{c2}=0.8194
Pressure ratio $\pi_c = 3.9$
Exit temperature T_{03_c2}= 501.88 K
Exit pressure P_{03_C2} = 804180 Pa
Power requested P_{c2}=48.71 kW</td></tr>
<tr><td><u>04-COMBUSTION CHAMBER</u>
Lower heating value H_u= 50 MJ/kg
Pressure loss factor f_c=2%
Efficiency η_{cc}=98%
Fuel flow rate $\dot{m}_{fuel} = 0.0064$ kg/s
Exit temperature T_{02}=1503 K
Exit pressure P_{04} =788100 Pa</td><td><u>05-TURBINE 1</u>
Polytropic efficiency η_{pol}= 85%
Isentropic efficiency η_{t1}=88.27%
Exit temperature T_{05}= 1353.3 K
Exit pressure $_{P05}$= 483490 Pa
Power generated P_{t1} =49.78 kW</td></tr>
<tr><td><u>05T2-TURBINE 2</u>
Polytropic efficiency η_{pol}=%85%
Isentropic efficiency η_{t2}= 88.27%
Exit temperature T_{05_T2}=942.04 K
Exit pressure P_{05_T2}= 58419 Pa
Power generated P_{t2} =165.55 kW</td><td><u>RECUPERATOR</u>
Effectiveness η_{rc}=90%
Pressure drop 4%
Exit temperature T_{03_rc}=888.97 K
Exit pressure P_{03_rc}= 804180 Pa</td></tr>
</table>

06-NOZZLE
Efficiency η_u=98%
Exit temperature T_6 = 925.44 K
Exit pressure P_{06} = 54014 Pa
Nozzle thrust T_{nozzle} =34.71 N
PERFORMANCE PARAMETERS:
Net power P_n= 126.82 kW
Available power P_{av} =100.0 kW
Chemical power P_c =321.42 kW
Fan thrust T_{fan} = 556.56 N (x2)
Total Thrust = 1147.8 N
Thermal Efficiency 39.46 %
Propulsive Efficiency 90.21 %
Total Efficiency 35.60 %
OTHER USEFUL PARAMETERS:
Bypass ratio 240.38
Pressure raise in fans $\Delta P/P_a = 0.023$
Air speed post fan V_{fan}=96.2 m/s
Mach post fan M_{fan} 0.3

Table 3.5: Parameters of the cycle selected

4 Centrifugal compressor design

The first and most important part to design in a gas turbine is the compressor. In our engine there are 2 centrifugal compressors with a pressure ratio of 3.9 each, for a total compression of 15.2, divided by an intercooler with the purpose of cooling the air flow thus reducing the diameter of the second compressor.

It has been decided to go with centrifugal compressors and not axial ones because they are easier to manufacture, they have a smaller cost for the same mass flow rate, they can reach a bigger pressure ratio (up to 5) with a single stage in respect to axial compressor stage that manage to compress only 1.2/1.5 times. Furthermore, these machines are less sensible to impurities in the sense that are less prone to be damaged by a foreign object and work better with dirty streams.

We choose to go with a bigger frontal area and higher weight, but on the other hand we have significantly reduced costs and failure hypothesis.

Before designing the low-pressure compressor, it is important to present the basic components and layout of this machine, in order to better understand the mechanics and the path followed by the air. In a centrifugal compressor the stream enters axially and is turned perpendicular to the axis of rotation it is then compressed by centrifugal force, collected, channeled and exits radially.

The compressor is composed by 3 parts as we can see in fig [1]:

- Impeller (rotor)
- Diffuser (stator)
- Volute (scroll)

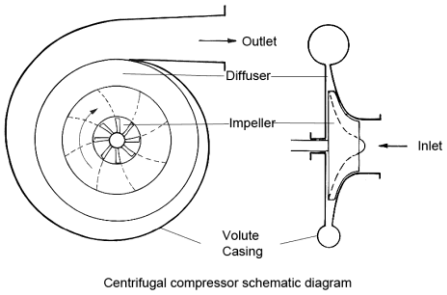

Figure 4.1: Centrifugal compressor parts

Before entering the rotating part, inlet guide vanes can be introduced to twist the flow and reduce the angle of attack, to avoid shocks, boundary layer separation, and in general any turbulence that can make the compressor to perform less well. Usually for small compressor these airfoils are not necessary.

The impeller is the rotating part connected by means of a shaft to the turbine that drives it, t's made of blades (usually in prime numbers), with the initial part (Inducer) that can be curved to better accommodate the airflow that enters the machine. His job is to accelerate the fluid outward from the centre of rotation and

conveying the energy from the turbine to the fluid, that in turn gets denser and hotter. Moreover, the blades can be radial or curved forward/backward to better conduce the flow and generate more power (we will see more about that later when designing).

The air exiting the rotor enters in the stationary part, or Diffuser, which it is necessary to slow the flow down and complete the compression. This part converts the kinetic energy of the air into potential energy. This section can be vaneless, vaned or mixed with a first part without blades and a second part where the flow is channelled and collected in channels or pipes.

The flow at this point enters the scoll where its collected in a unique stream and continue his journey to the intercooler or the combustion chamber.

4.1 Low-pressure compressor

We want to design our two turbomachines to be as efficient as possible when they work at cruise speed, as studied before in this paper. To do so, we present once more the basic parameters at the entrance and exit of the first compressor stage.

- Total inlet Temperature T_{01}= 259.47 K
- Total inlet Pressure P_{01}=56812 Pa
- Flow density ρ=0.6624 Kg/m^3
- Mass flow rate $\dot{m}$=0.2631 Kg/s
- Total exit Temperature 411.35 K
- Total exit Pressure 221500 Pa

To proceed with the preliminar design of the turbomachine it is necessary to assume a few project parameters:

- After few tries it has been decided to proceed without inlet guided vanes because the angular change of the flow was really small (in the order of 5°) and there wasn't a significant change of other parameters. Thus, in order to keep the machine simple and the costs as low as possible, the flow will enter axially. C_{1t}=0 C_1=$C_{1\ axial}$
- After some shaft considerations the hub diameter of the impeller has been imposed to be 16 mm
- To decide the rotational speed few electric high-speed generators have been looked up, in particular, at the reference [5] it is stated that for

permanent magnets generator, the speed for a 100kW motor cannot exceed 60000 rpm, unless a massive stainless steel rotor is used. Thus, using the best generator on the market, we decided to use 60000 rpm (or 1000 rev/s) as rotational speed

- Number of blades *n* =15
- Pressure losses equal between impeller and diffuser $\eta_{impeller} = 0.5 \cdot (1 + \eta_c)$
- Power input factor ψ= 1.035

Remember that Gas properties (cp e k) are calculated as showed in Appendix A, using an empirical correlation with the temperature, at each step.

Having set these parameters, we proceed creating a MATLAB program able to calculate the dimensions of the parts, the velocity triangles, and the thermodynamic parameters at each stage. Hereunder we are going to describe every step and the formulae we used for a better understanding of the process. It is started by calculating every parameter for a radial blade impeller then it will be transformed if necessary to accommodate backward leaning blades.

4.1.1 Impeller

First, we want to find how high the total velocity that enters the impeller is, knowing that C_1=C_{1ax} and using the mass flow rate equation conveniently modified to calculate the velocity at the impeller inlet tip we obtain:

$$C_{1ax\_t} = \sqrt{R \cdot T_{01} \cdot \frac{k \cos\beta 1t^2 \left[1 - \frac{k-1}{2k}\left(\frac{C_{u1t}}{\sqrt{RT_{01}}}\right)^2\right] M_{1\,rel}^2}{\left[1 + \frac{k-1}{2}\cos\beta 1t^2\, M_{1\,rel}^2\right]}} \qquad (4.1)$$

Where with B_{1t} we define the inlet blade tip angle, chosen equal to 50° (maximum), and M_{1rel}=0.8, to prevent flow separation at the entrance of the impeller. Assuming the entrance total velocity to be the same everywhere C_1 is now a known parameter.

We continue calculating the diameter of the impeller inlet tip, from the definition of mass flow:

$$D_{1t} = \sqrt{\frac{\dot{m}/\rho}{\frac{C_{1ax\_t} \cdot \pi}{4}} + D_{1h}^2} \tag{4.2}$$

Then, rearranging the pressure ratio definition we manage to calculate the rotational speed at the exducer:

$$U_2 = \sqrt{\frac{cp \cdot T_{01} \cdot \left(\pi_c^{\frac{k-1}{k}} - 1\right)}{\sigma \cdot \psi \cdot \eta_c}} \tag{4.3}$$

where σ is the slip factor for an impeller with radial blades. The following empirical formula derived by Staintz as:

$$\sigma = 1 - \frac{0.63 \cdot \pi}{n} \qquad with \quad n = number\ of\ blades \tag{4.4}$$

Consequently, knowing the rotational shaft speed the diameter at impeller outlet is obtainable.

$$D_2 = \frac{U_2}{\pi \cdot rps} \tag{4.5}$$

Another way to calculate this quantity, if the shaft rotational speed was unknown, was to use the following assumption:

$$\frac{D_2}{D_{1t}} = \frac{U_2}{U_{1t}} \quad \rightarrow \quad \frac{D_2}{D_{1t}} = \frac{\frac{U_2}{\sqrt{RT_{01}}}}{\frac{C_{1ut}}{\sqrt{RT_{01}}} + \frac{C_{1ax}}{\sqrt{RT_{01}}} \tan \beta_{1t}} \tag{4.6}$$

and then trace back and calculate the RPM with an inverse formula.
Done that it's easy to determine the inlet area A_1 and as a consequence, the thermodynamic properties and the velocity triangles at the inlet hub, tip and mean radius (shown in Figure 4.2)

$$T_1 = T_{01} - \frac{C_1^2}{2 \cdot cp} \qquad \frac{P_1}{P_{01}} = \left(\frac{T_{01}}{T_1}\right)^{\frac{k}{k-1}} \qquad \rho_1 = \frac{P_1}{R \cdot T_{01}} \tag{4.7}$$

$$M_1 = \frac{C_1}{\sqrt{k \cdot R \cdot T_1}} \qquad M_{1rel} = \frac{W_1}{\sqrt{k \cdot R \cdot T_1}} \tag{4.8}$$

To simplify the reading all the results are written in Table 4.1-2.

Table 4.1: Thermodynamical data impeller inlet

Thermodynamic data	
T_1 [K]	245.06
P_1 [Pa]	46585
ρ_1 [kg/m^3]	0.6624
A_1 [m^3]	0.0023
M_1	0.5394
$M_{1\ rel}$	0.784

Table 4.2: Geometry dimensions impeller inlet

Geometry and velocity data	
C_1 [m/s]	169.50
W_1 [m/s]	246.38
U_{1h} [m/s]	50.27
U_{1t} [m/s]	178.81
U_2 [m/s]	410.5
D_{1h} [mm]	16
D_{1t} [mm]	57
D_2 [cm]	13,07

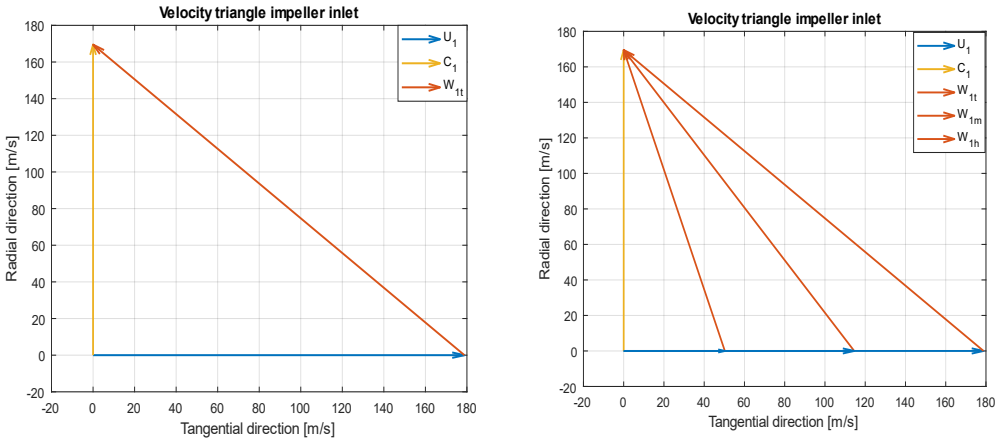

Figure 4.2: Velocity riangles Impeller inlet

Now we can proceed with the calculation of the flow leaving the impeller. Once again, the fact that we are doing the calculation for a radial blade impeller needs to be underlined.

Thermodynamic properties of the fluid are calculated imposing the maximum exit Mach number M_2=1 that allows us to find C_2 easily. From previous cycle calculation we know T_{02} (that is equal to T_{03} at the exit of the diffuser, because the latter doesn't do any work so the total quantities remain unchanged), therefore using few simple equations and some trigonometric we find T_2, P_2, ρ_2, C_2 and all the velocities. The height of the passage b_2 is now calculated using the mass flow rate.

$$b_2 = \frac{\dot{m}}{\rho_2 \cdot C_{2r} \cdot \pi \cdot D_2} \tag{4.9}$$

We had noticed that the flow exits the impeller with a certain angle with respect to the radial blades, if we imagine to perfectly guide the flow to the exit, we should obtain that $C_{u2}=U_2$, and therefore a perfect outlet velocity triangle and high efficiencies. In practice this cannot be done because it would take an infinite number of blades. But we can guide the flow with backward leaning blades in order to achieve a smaller C_2 at the exit of the impeller and higher efficiencies for the impeller.

The decrease of absolute velocity C_2, makes easier for the diffuser to do his job, and allows the compressor to have a wider operating range at that rotational speed, for a better matching with the turbine.

Assumed that, to use backswept blades, we want the same pressure ratio between backward leaning and radial impeller, we can match the two equations obtaining a fresh relationship of $U_{2backward}$ with $U_{2radial}$, and since the diameter of the impeller D_2 varies linearly with the velocity, the diameter $D_{2backward}$ is obtained, through which all the other quantities can be updated.

$$\left(\frac{U_{2backward}}{U_{2radial}}\right)^2 = \frac{\sigma}{\sigma_{backward}\cdot(1-\varphi_2\cdot\tan\beta_2)}$$
$$with\ \sigma_{backward} = 1-\frac{\frac{0.63\pi}{n}}{(1-\varphi_2\cdot\tan\beta_2)} \qquad \varphi_2 = \frac{C_{2r}}{U_2} \tag{4.10}$$

We represent in Figure 4.3 the velocity triangles on the radial plane at the outlet of the impeller.

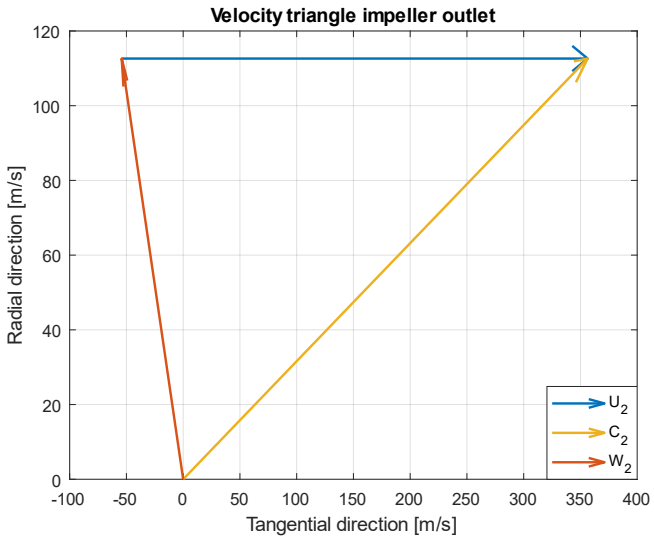

Figure 4.3: Velocity triangle impeller outlet

Table 4.3: Quantities at impeller outlet for backward blades

Quantities at impeller outlet			
$\sigma_{backward}$	0.846	β_2 [°]	30
C_{2r} [m/s]	112.61	α_2 [°]	16.31
C_{2u} [m/s]	384.66	$D_{2backward}$ [m]	0.1431
C_2 [m/s]	400.81	b_2 [m]	4.6
W_2 [m/s]	203.87	T_2 [K]	343.39
U_2 [m/s]	449.68	P_2 [Pa]	132950
M_2 []	1.081	ρ_2 [Kg/m^3]	1.349

Before we look at the diffuser, it's necessary to calculate the axial length of the impeller, in order to have the complete geometry of the part. After some research, a correlation between the outlet diameter and the axial length of the turbomachine has been found in the studies conducted by Aungier [6] which is the following:

$$L = D_2 \cdot \left(0.014 + 0.028\left(\frac{D_2}{D_{1h}}\right) + 1.58\varphi\right)$$
$$with \quad \varphi = \frac{4Q_0}{\pi U_2 D_2^2}, \quad Q_0 = \frac{\dot{m}}{\rho} \tag{4.11}$$

For our low-pressure compressor, we found L=4.13 cm, fairly consistent with the other geometrical parameters of the impeller.

4.1.2 Diffuser

As said before, the diffuser can be vaneless or vaned. There are a few types of vaned diffuser such as pipe diffuser, wedge, cascade, with pivoting vanes, and so on. Usually this are more efficient and compact because they can decelerate the fluid in less space, but they are more difficult to design, and CFD simulations are usually required to obtain adequate dimensions without compromising the fluid motion. Additionally, their production cost is higher, therefore it has been decided to initially opt for a vaneless diffuser even if slightly bigger.

The main hypothesis done in this case is that the absolute velocity at the exit of the diffuser is equal to the one entering the inlet of the impeller (C_3=C_1), and that the height of the diffuser remains the same b_2=b_3. Observing that the diameter varies

linearly with the speed, D_3 can be easily calculated and therefore also thermodynamic properties.

$$D_3 \cdot C_3 = D_2 \cdot C_2 \tag{4.12}$$

We present the results down here in Table 4.4.

Table 4.4: Quantities at diffuser outlet

Quantities at DIFFUSER outlet			
C_{3r} [m/s]	77.58	**A_3 [m^3]**	0.0045
C_{3u} [m/s]	150.70	**D_3 [m]**	0.3090
C_3 [m/s]	169.50	**T_3 [K]**	397.15
M_3 []	0.425	**P_3 [Pa]**	199850
α_3[°]	10.71	**ρ_3 [Kg/m^3]**	1.753

Pressure coefficient C_{pr} and degree of reaction are also calculated.

$$Cp_r = \frac{P_3 - P_2}{P_{02} - P_2} = 0.5651 \qquad \Lambda = \frac{T_2 - T_1}{T_3 - T_1} = \quad 64.7\% \tag{4.13}$$

The pressure recovery coefficient states what portion of total pressure is recuperated in the diffuser. It is difficult to reach high values, and the one obtained here can be considered good.

The degree of reaction is the ratio of the work done by reaction to the total work done in the compressor. If you have a value of 100% the whole enthalpy increment happens in the rotor, and the stator only turns the absolute velocity. Vice versa if $\Lambda = 0$ the rotor changes the kinetic energy only, and this is then recuperated in the diffuser. Usually, you try to have a value around 50% so that the total enthalpy variation is done half by the rotor and half by the stator. Even though in our case most of the work is done in the rotor, our value can be considered acceptable.

4.1.3 Vaned diffuser

Introducing a lot of hypotheses, a vaned diffuser has also been developed, with an initial vaneless part and a 16-vanes wedge diffuser.

Following the design done by Aungier in his book [6] the subsequent constraints have been adopted:

- D_3/D_2 =1.125
- β_3=16°
- $2\theta_c$=8°
- Length to width ratio=10 (fig. [4])
- D_4/D_3 =1.4

With the subscript 3 we indicate the diameter of the vaneless space, and with 4 the diameter of the vaned space, and therefore the total diameter.

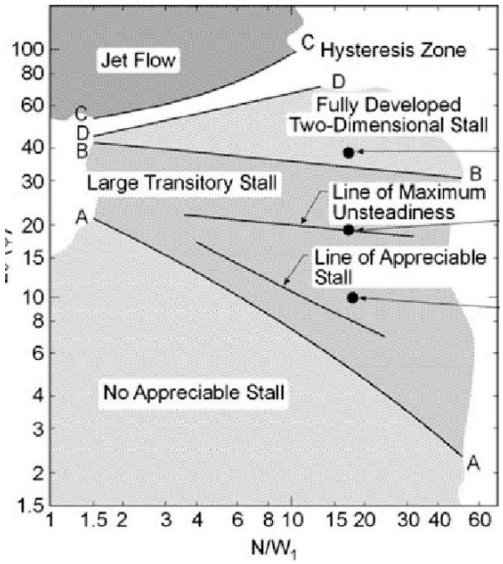

Figure 4.4: Diffuser stall conditions

This allowed us to calculate through simple equations the main parameters of a wedge diffuser, using the equation below:

$$W_{throath} = \frac{\pi \cdot D_3 \cdot \sin \beta_3}{n_{vanes}} \tag{4.14}$$

$$AR = \frac{W_{exit}}{W_{throath}} = 1 + 2 \cdot LWR \cdot \tan \vartheta_c \tag{4.15}$$

$$\beta_4 = \sin^{-1}\left(\frac{n_{vanes} \cdot W_{exit}}{\pi \cdot D_4}\right) \tag{4.16}$$

Then inverting the following equations, we find the Mach number, at the exit of the vaned section.

$$AR = \frac{1}{M} \cdot \left(\frac{2}{k-1} \cdot \left(1 + \frac{k-1}{2} M^2\right)\right)^{\frac{k+1}{2(k-1)}} \tag{4.17}$$

Thermodynamic properties and other quantities are calculated as before.

Table 4.5: Quantities at Vaned Diffuser outlet

Quantities at Vaned Diffuser outlet			
C_{4r} [m/s]	100.8	**A_4 [m^3]**	0.0033
C_{4u} [m/s]	1.107	**D_4 [m]**	0.2254
C_4 [m/s]	100.85	**T_4 [K]**	406.26
M_4 []	0.25	**P_4 [Pa]**	205630
β_4[°]	28.18	**ρ_4 [Kg/m^3]**	1.763
Cp_r[]	0.6140	Λ [%]	61.0

As could be seen from the results written in Table 4.5 the diameter of the diffuser is smaller in this case as expected, thus reducing the frontal area of the compressor, and probably the weight too. The outlet mack number is 0.25 that is perfect to enter the combustion chamber as it is not too high to blow off the flame or the intercooler. Thermodynamic properties remain almost unchanged, and we have a small variation in the pressure recovery coefficient and in the degree of reaction, with the vaned diffuser recuperating a bigger part of kinetic energy in respect to the vaneless one.

4.2 High-Pressure Compressor

4.2.1 Single shaft configuration

A similar path has been followed to estimate the geometrical dimensions and gas properties of the second compressor. Here we report the initial assumption and the thermodynamic quantities at the inlet.

- Total inlet Temperature T_{01}= 317.93 K
- Total inlet Pressure P_{01}=214860 Pa
- Flow density ρ=2.32 Kg/m^3
- Mass flow rate $\dot{m}$=0.2631 Kg/s
- Total exit Temperature 501.88 K
- Total exit Pressure 804180 Pa

One main constraint is that we want the same rotational speed of the first compressor because they are both attached to the same shaft, and we want the Mach number at the exit of the diffuser to be smaller than 0.4 to assure that the flow enters the combustion chamber at the right speed.

At the impeller inlet we obtain the following results and velocity triangles, down here are also presented the main geometrical quantities of the impeller.

Table 4.6: Geometry and velocity data HP impeller

Geometry and velocity data	
C_1 [m/s]	59.69
W_1 [m/s]	173.04
U_{1h} [m/s]	50.27
U_{1t} [m/s]	12.41
U_2 [m/s]	106.34
D_{1h} [mm]	16
D_{1t} [mm]	51
D_2 [cm]	14.45
L [cm]	3.55

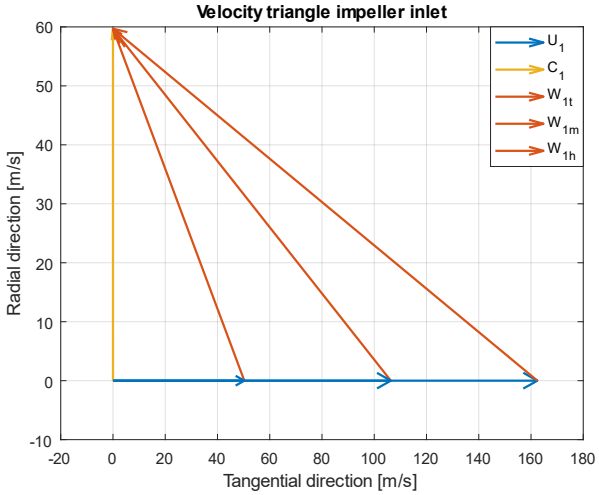

Figure 4.5: Velocity triangles HP impeller inlet

In Table 4.7and Figure 4.6 are listed the results for the impeller outlet, with back-swept blades.

Table 4.7: Quantities at HP impeller outlet

Quantities at impeller outlet			
$\sigma_{backward}$	0.8466	**β_2 [°]**	30
C_{2r} [m/s]	120.03	**α_2 [°]**	15.72
C_{2u} [m/s]	426.35	**$D_{2backward}$ [m]**	0.1578
C_2 [m/s]	442.93	**b_2 [m]**	0.0013
W_2 [m/s]	222.46	**T_2 [K]**	420.52
U_2 [m/s]	495.65	**P_2 [Pa]**	505300
M_2 []	1.08	**ρ_2 [Kg/m^3]**	4.1867

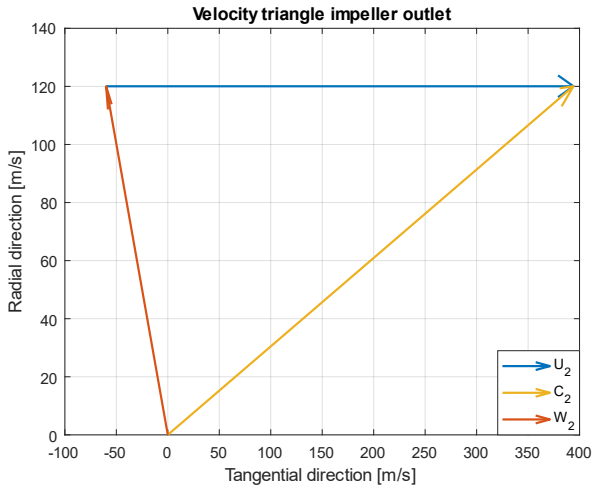

Figure 4.6: Velocity triangle HP impeller outlet

Lastly, we present the results for vaneless and vaned diffuser.

Table 4.8: Vaneless and Vaned diffuser outlet HP compressor

Quantities at Vaneless Diffuser outlet				**Quantities at Vaned Diffuser outlet**			
C_{3r} [m/s]	80.38	**A3 [m^3]**	0.0014	**C_{4r} [m/s]**	111.0	**A_4 [m^3]**	0.00098
C_{3u} [m/s]	156.66	**D3 [m]**	0.3635	**C_{4u} [m/s]**	1.2205	**D_4 [m]**	0.2485
C_3 [m/s]	176.08	**T_3 [K]**	486.81	**C_4 [m/s]**	111.06	**T_4 [K]**	495.81
M_3 []	0.4	**P_3 [Pa]**	768520	**M_4 []**	0.25	**P_4 [Pa]**	769870
α_3[°]	10.18	**Rho_3 [Kg/m^3]**	5.50	**β_4[°]**	28.18	**ρ_4 [Kg/m^3]**	5.41
Cp_r[]	0.5886	**Λ [%]**	61.16	**Cp_r[]**	0.5916	**Λ [%]**	58.9

Looking at the results, they are consistent with the ones of the low-pressure compressor, with similar dimensions, and the second stage slightly bigger than the first stage. These dimensions would have been even bigger without the intercooler in between, due to the higher temperature, the impeller would have taken a bigger room to compress the fluid of the right amount.

All the thermodynamic quantities are consistent with the cycle analysis done in the first chapters.

4.2.2 Double shaft configuration

Since the dimensions of the second compressor are slightly bigger than the first, partially compromising the use of the intercooler, that was adopted with the aim of reducing compressors geometries. We tried to change configuration, using two concentric parallel shafts with different rotating speed, allowing the high-pressure compressor to rotate faster. This should result in a smaller diameter of the rotor and thus the entire compressor itself.

We report down below the results obtained with the same entrance quantities as before.

- *Rotor inlet*:

Table 4.9: Geometry and main data HP 2 shaft configuration

Geometry and velocity data	
C_1 [m/s]	59.69
W_1 [m/s]	221.59
U_{1h} [m/s]	99.77
U_{1t} [m/s]	213.40
U_2 [m/s]	495.66
D_{1h} [mm]	0.026
D_{1t} [mm]	0.0556
D_2 [cm]	11.83
L [cm]	2

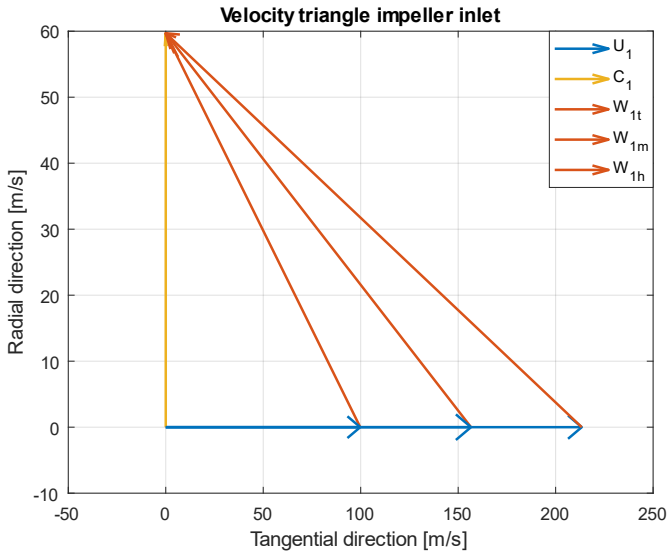

Figure 4.7:Velocity triangles HP impeller 2-shaft configuration

- *Impeller outlet with backward-leaning blades*:

Table 4.10: quantities HP impeller outlet 2-shafts configuration

Quantities at impeller outlet			
$\sigma_{backward}$	0.466	β_2 [°]	30
C_{2r} [m/s]	120.04	α_2 [°]	15.72
C_{2u} [m/s]	426.35	$D_{2backward}$ [m]	12.92
C_2 [m/s]	442.93	b_2 [m]	0.0015
W_2 [m/s]	222.46	T_2 [K]	420.52
U_2 [m/s]	495.66	P_2 [Pa]	505300
M_2 []	1.08	ρ_2 [Kg/m^3]	4.188

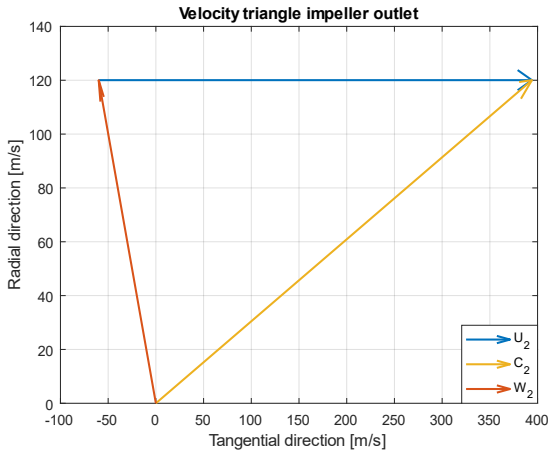

Figure 4.8: Velocity triangle HP impeller outlet 2-shaft configuration

- *Vaned diffuser outlet section*:

Table 4.11:Quantities at diffuser HP outlet 2-shafts configuration

Quantities at Vaned Diffuser outlet			
C_{4r} [m/s]	111.0	A_4 [m^3]	0.0009828
C_{4u} [m/s]	1.22	D_4 [m]	0.2034
C_4 [m/s]	111.06	T_4 [K]	495.81
M_4 []	0.25	P_4 [Pa]	769870
β_4[°]	28.18	ρ_4 [Kg/m^3]	5.41
Cp_r [ ]	0.5916	Λ [%]	58.09

As can be seen see from the results obtained, there is a clear difference between the two configurations, with the second one (twin spool configuration) that allow for a smaller HP-compressor. In total, we save about 6 cm in diameter but there are higher mechanical stresses acting on the shaft due to the higher rotational speed (78833 RMP), and the wear would be much more elevated.

4.2.3 Configuration selection

To choose the correct configuration for the gas turbine, we look at compressors machine numbers plotting them in a pump chart. The two numbers used are respectively, Specific Speed and Specific Diameter, both dimensionless.

$$N_s = \frac{rpm \cdot \sqrt{Q}}{\Delta H^{3/4}} \tag{4.18}$$

$$D_s = \frac{D \cdot \Delta H^{1/4}}{\sqrt{Q}} \tag{4.19}$$

With Q volumetric flow rate and D impeller exit diameter.

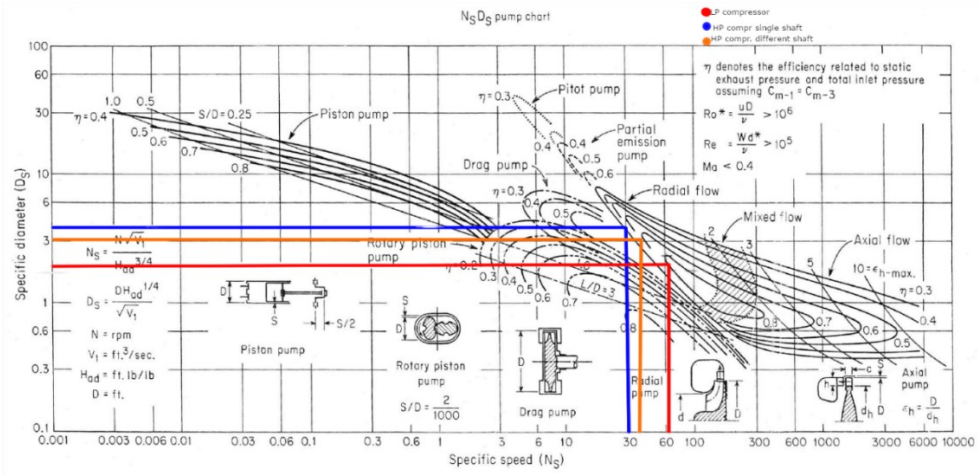

Figure 4.9: Pump chart with machine number displayed [24]

A we can see from Figure 4.9, the low-pressure compressor (red line on the graph) hits exactly the 0.8 total-to-static efficiency curve for radial compressors. Since our isentropic efficiency is 0.8194 for both compressors, calculated from the polytropic one, and remembering that the following relation is valid.

$$\eta_{ic} = \eta_{ts,c} - \frac{C_4^2}{2 \cdot cp \cdot (T_{01} - T_{04})} = 0.79 \qquad (4.20)$$

We can say that the choice of a radial compressor for the low-pressure stage is the correct one.

The high-pressure compressor can be displaced in two configurations as seen before, with the first one plotted in blue, that has the rotor on the same shaft of the first stage and the RPM fixed at 60000.

The second configuration instead, has the second compressor placed on another shaft parallel to the first one that spins at an higher speed (78833 rpm), allowing the whole stage to be smaller.

This design is plotted in orange in Figure 4.9.

We see that both configurations are on different efficiency curves, and at the limit of the radial flow usage area. Nevertheless, the two-shaft configuration seems to be the best one with a higher efficiency near to the one calculated that is about $\eta_{ts,c}$=0.78.

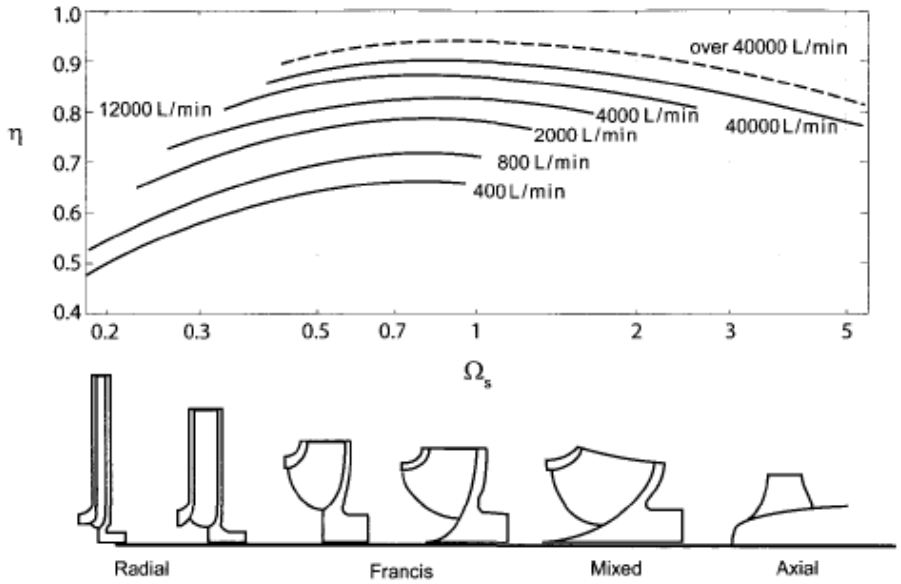

Figure 4.10: Geometrical configuration of the impeller based on Specific speed [7]

Moreover, if we look at the graph in Figure 4.10, we can confirm the dimensions calculated before, with the first compressor that has a deeper impeller in the axial direction (like the Francis type in the figure), while the second one due to a smaller

specific speed, here called Ω_s, resemble the radial type, being a little bit more compact axially.

The choice falls back to the two parallel-axis configurations due to higher efficiencies and smaller dimensions of the rotative parts.

4.3 Material selection

Knowing all the measures and the quantities necessary, we now proceed with the selection of the material to be use for both compressors. Nowadays the choice of the material, not only is a question of finding the best material with the most ideal properties, but costs per unit, availability and ease of production are important factors to be taken into account. The choice of materials to be used in both impeller and diffuser of a compressor, requires a selection based on a multitude of material properties that we are going to list below:

- Tensile/Yield strength
- Elastic modulus
- Thermal expansion coefficient
- Fracture toughness
- Fatigue strength
- Impact resistance
- Dampening
- Machinability
- Ductility
- Corrosion and erosion resistance

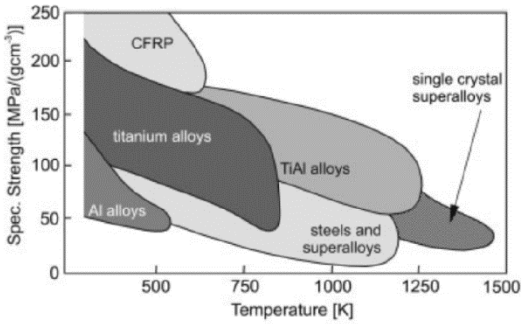

Figure 4.11: Specific strength of materials over Temperature

Nowadays, most of the Centrifugal compressors for ground and aeronautical application are made of Stainless Steel (usually AISI 400) with a better corrosion resistance thanks to the lower amount of carbonium and the presence of chromium in the alloy (Maraging steels and AerMet 100 are a good example). Other materials used are titanium and titanium alloys that presents a higher strength to density ratio for the range of temperature we are interested in. This can be seen in Figure 4.11.

Axial compressor stages use only Titanium for the blades because it offers great mechanical properties and creep resistance at high temperatures. Boeing with the 787 decided to innovate in this sector using blades made of Titanium aluminide that offers excellent corrosion and oxidation resistance at high temperature and low weight. This material can also be produced with additive manufacturing techniques, hence reducing production costs.

On the other hand, its direct competitor is an Aluminium alloy made by Airbus, called Scalmalloy. This material has optimum qualities and material properties up to 250 °C (573 K), perfectly in the range of temperature of our compressors. With a low thermal expansion, high resistance to mechanical stresses, good corrosion resistance and low weight it is a suitable candidate for our parts. Additive manufacturing fabrication allows to contain the costs of production made high by the presence of Scandium in the alloy

For our compressors, if we don't focus on the costs of the material, we are surely choosing Titanium or Aluminium because they offer better mechanical properties, corrosion resistance and low thermal expansion, all combined with a lower density and therefore lower weight than steel. Grade 5 Titanium (Ti6Al4V) would probably be the best choice, to be evaluated with Titanium aluminide (TiAl).

Lower weight and ease to manufacture make us propend to use Scalmalloy, but the variation of the mechanical properties with temperature and fatigue wear needs to be analysed to avoid in-use breaks.

A mechanical stress calculation has been carried out to see if the chosen materials could sustain the high tensions generated during the operations on disk and blades. To evaluate that we use two empirical formulae found at the reference [8]. The first one is to evaluate the maximum peak disc stress, while the second one estimates the stress on the blades.

$$\sigma_{\max disc} = 0.75 \cdot \rho \cdot U_2^2 \cdot \frac{3 + \nu}{8} \qquad with\, \nu = Poisson'sRatio \tag{4.21}$$

$$\sigma_{\max blade} = \frac{6 \cdot f \cdot b_2^2 \cdot \rho \cdot \omega^2 \cdot \sin\beta_2}{t_{tip}} \tag{4.22}$$

(f is an empirical parameter chose to be 0.167 as suggested in reference [4], t_{tip} is the blade thickness set at 1 mm)

As we can see from Table 4.12, for the high-pressure compressor (the one subjected to higher stresses) maximum stress values remain well under the yield strength of the material that is around 1100 Mpa for Titanium at 500°C. The same considerations can be done for the Aluminium alloy which has a yield strength of 470 Mpa.

Table 4.12: stresses on disk and blades per material

	Grade 5 Titanium
$\sigma_{\max disc}$ **[MPa]**	284.98
$\sigma_{\max blade}$ **[MPa]**	138.86

	Scalmalloy
$\sigma_{\max disc}$ **[MPa]**	188.40
$\sigma_{\max blade}$ **[MPa]**	138.86

This is to be considered a preliminary analysis, with the only purpose to check if the material is strong enough to handle the stresses. A FEM simulation would be a better way to evaluate mechanical stresses and needs to be done before the final choice of the material.

5 Turbine design

After the design of both radial compressors, we must look at the turbines that are the most important part of a gas engine because they convert the energy stored inside the fluid after it has passed through the combustion chamber, into rotational energy used to drive the compressor and then the alternator that will power our aircraft.

In aeronautical engines, two types of turbines can be used, Axial turbines and radial inflow ones. We are incline to use the latter because they bring lots of benefits such as: higher efficiencies for low power outputs, high reliability, better efficiencies at off design conditions and can handle in a better way the small mass flow rate requested for this application. They are also easy to manufacture, smaller and cheaper than the axial ones. On the other hand we are faced with an hard to cool down and difficult to be put in series machine.

To check if radial turbines are suitable for our purposes, and to check which, between the various setups of generators is the best to be used in our situation, we plot the machine numbers Ns (specific speed) and Ds (specific diameter) on a turbine chart. These numbers are calculated as previously done in the compressor design chapter.

5.1 Machine numbers and configuration selection

5.1.1 Generator on LP-shaft

As seen the configuration used presents the following Specific speed and diameter, reported in Table 5.1.

Table 5.1: Machine numbers 1st configuration

Machine numbers	LP turbine	HP turbine
Ns	17.89	47.01
Ds	6.05	2.30
Efficiency	0.4	0.8

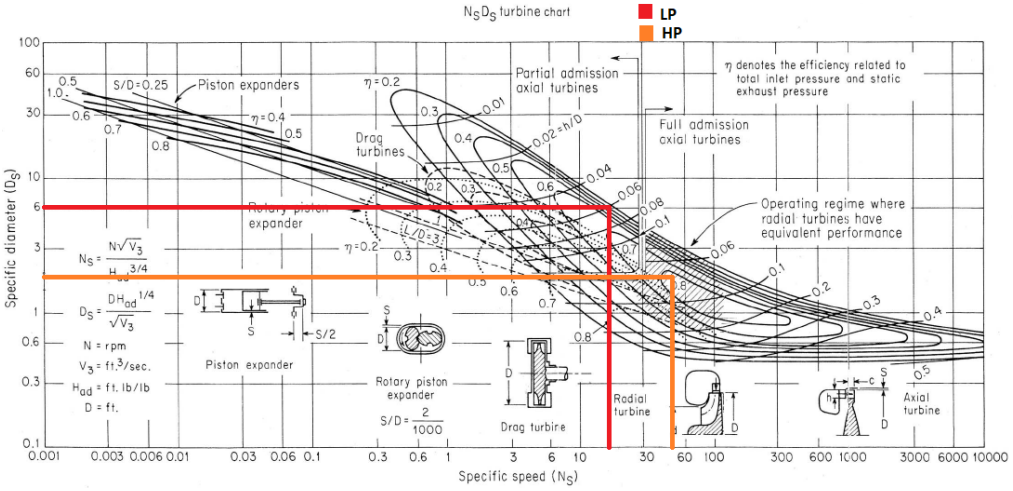

Figure 5.1: Turbine chart for generator on LP-shaft: HP in orange, LP in red

We can see from Figure 5.1 the high-pressure turbine falls exactly in the radial turbine section of the chart, and it seems to have a correct total-to-total efficiency value around 0.8. We can calculate this efficiency by means of the following formula:

$$\eta_{t,t} = \frac{1}{\frac{1}{\eta_{it}} + \frac{C_3^2}{2 \cdot cp \cdot (T_{01} - T_{03})}} \tag{5.1}$$

In the first place, with the data we own, this efficiency value is about 0.83, similar to the one found in the chart. The low-pressure turbine instead presents a low value of specific speed, causing the efficiency to be distant from the one calculated, but still inside the usage of the radial turbine instead of the axial ones.

5.1.2 Generator on HP- shaft

In the second configuration possible the generator is keyed on the high-pressure shaft, with the corresponding turbine that drives it, while the LP-turbine drives the compressor only.

Down here are reported machine numbers and turbine chart.

Table 5.2: Machine numbers 2nd configuration

Machine numbers	LP turbine	HP turbine
Ns	102.55	18.33
Ds	1.05	5.91
Efficiency	0.8	0.4

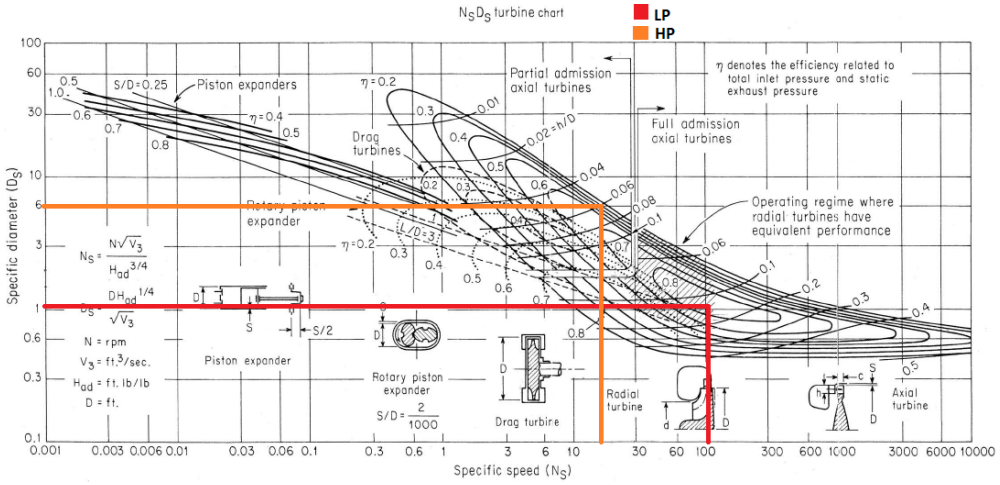

Figure 5.2: Turbine chart for generator on HP-shaft: HP in orange, LP in red

We can see that the chart is similar to the one presented above, with machine numbers inverted between the two stages. The low-pressure turbine has an efficiency of 0.8 exactly centred on the radial turbine usage. On the other hand, the high-pressure turbine due to the work needed to spin the generator has a smaller specific speed and higher specific diameter that brings the efficiency down, at values around 50%, as similarly done in the previous setup.

5.1.3 Two-generators configuration

The last configuration analysed is the one with two generators, one for each shaft, connected in parallel.

Table 5.3: Machine numbers 3rd configuration

Machine numbers	LP turbine	HP turbine
Ns	31.81	26.36
Ds	3.41	4.11
Efficiency	0.5	0.5

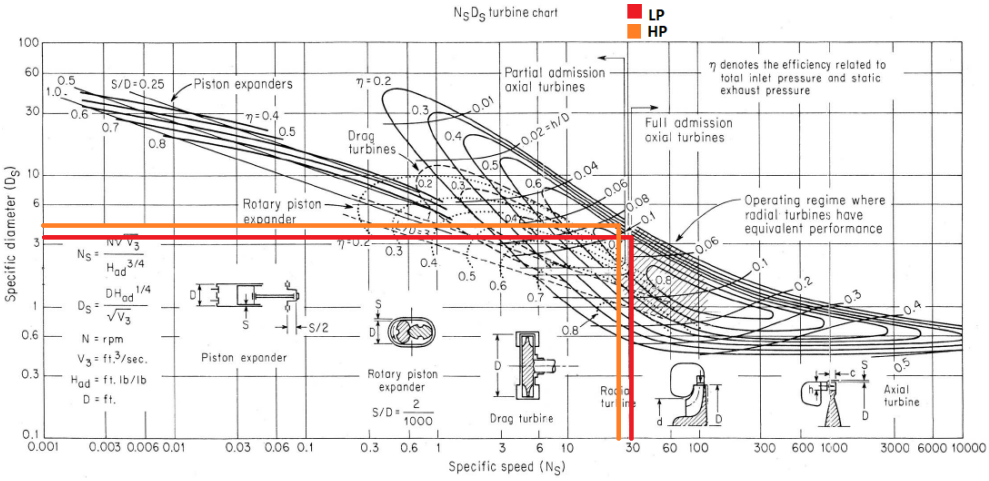

Figure 5.3: Turbine chart for generator on both shafts: HP in orange, LP in red

In this case the numbers are similar to each other, so it looks like this is the most balanced setup. But due to the power drawn from the generators, the efficiencies found in the graph are far from the ideal ones we want for our turbines, with values between 0.4 and 0.5.

5.1.4 Final considerations

In my opinion, the last arrangement can be excluded seen the lower values of the efficiencies, and the fact that two generators are bulkier and difficult to be operated in parallel. The choice needs to be done between the first two setups, that are similar to one another, with at least one turbine at the desired efficiency. At this point the implementation of the first one instead of the second one, falls back to overall dimensions, weights, and efficiencies of the generator, with one that is clearly preferrable as discussed in the previous comparison.

Therefore, two radial inflow turbines will be used, the first one will only be used to spin the HP-compressor, while the second one will provide also the power needed to run the electric generator.

5.2 General geometry

As can be expected, the geometry of a radial inflow turbine is very similar to the compressor one, but the fluid, in this case combustion gasses, enters from the volute passes through the stator/nozzle vanes which provides the right angular momentum and accelerates the flow at the right speed. The combusts then encounter the rotor which will be forced to spin thus reducing the pressure of the fluid and as a result the temperature. Blades are usually straight and radial. All these parts are showed in Figure 5.4.

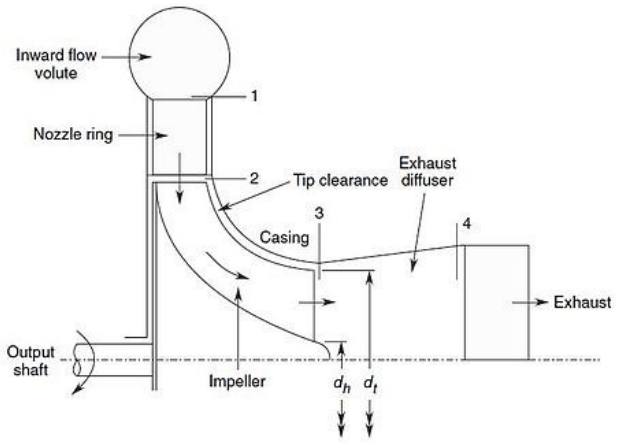

Figure 5.4: Geometry of a turbine impeller

The flow exits axially at lower radius, making a 90° turn, and is channelled to go to the next stage or into a nozzle that accelerate the air providing, in our case, a little bit of thrust. There can be a little diffuser downstream the rotor to slow the fluid down to a usable value.

5.3 High-pressure Turbine

We want our turbine to be as efficient as possible, and in this paragraph we are going to define the main geometrical characteristic of the turbomachine and the thermodynamic properties at each step to ensure a high efficiency engine.

The high-pressure turbine is the first thing the fluid encounter after the combustion chamber, it is keyed on the same shaft of the compressor, hence it has the same rotational speed.

We present down here the main parameters at the entrance and exit of the turbine:

- Total inlet Temperature T_{01}= 1503 K
- Total inlet Pressure P_{01}= 788100 Pa
- Flow density ρ= 1.743 Kg/m^3
- Mass flow rate $\dot{m}$=0.2695 Kg/s

- HP compressor power 49.788 kW
- 78833 rpm

Cp, k and R are calculated at each step as seen on Appendix A.

In order to start the preliminary design, we have to define few dimensionless parameters that we will use:

- *Stage Loading*: it is a measure of the load on a turbomachine, and it is defined as in the equation below, with the right term that is negligible

$$\psi = \frac{C_{2u}U_2 - C_{u3}U_3}{U_2^2} \approx \frac{C_{2u}}{U_2} = 0.8 \div 1 \tag{5.2}$$

  We will choose a value of 1.
- *Flow coefficient*:

$$\Phi = \frac{C_{3a}}{U_2} = 0.3 \div 0.4 \tag{5.3}$$

  We will choose a value of 0.35.
- *Rotor meridional velocity ratio*:

$$\xi = \frac{C_{2r}}{C_{3a}} \approx 1 \tag{5.4}$$

Other two parameters that we are going to use are:

- $\frac{r_{3h}}{r_2} = 0.25$
- $\eta_{tt} = 0.88$

5.3.1 Design steps

These steps follow the design process found in reference [9].

Knowing the power that needs to be generated from this turbine because it is equal to the power requested from the compressor, the enthalpy drop can be calculated and therefore the exit temperature can be found.

$$P = \dot{m}_c \cdot cp \cdot (T_{01} - T_{03}) \;\rightarrow\; T_{03} = T_{01} - \frac{P}{cp \cdot \dot{m}_c} \tag{5.5}$$

The rotor tip speed U_2 also derives from the enthalpy drop, and remembering the flow coefficient formula, the exit axial speed C_{3a} is found:

$$U_2 = \sqrt{\Delta H} \qquad C_{3a} = \Phi \cdot U_2 \tag{5.6}$$

Here an approximation is done defining C_3=C_{3a} thus imposing that the flow exits the rotor completely axial and without any swirl.

Now we assume the blades to be radial at the inlet of the rotor because they provides the best condition with respect to stressing. Usually in this case is then assumed that the inlet relative velocity is aligned with the blades (to obtain the best efficiency) thus imposing $\psi = 1$ and therefore β_2=0, obtaining a simple right velocity triangle at the inlet. But as said in reference [10] it has been shown that a significant incidence angle occurs in this case. In the same paper a formula for the absolute and relative velocity angles is obtained in function of the number of blades (in our case 15):

$$\cos \alpha_2 = \frac{1}{\sqrt{n}} \qquad \beta_2 = 2 \cdot (90° - \alpha_2) \tag{5.7}$$

We can now redefine the stage loading as $\psi = \cos \beta_2$. This will allow us to calculate the velocity at the inlet and therefore plot our velocity triangles.

$$C_{2u} = \psi \cdot U_2 \qquad C_{2r} = \xi \cdot C_{3a}$$
$$thus \quad C_2 = \sqrt{C_{2u}^2 + C_{2r}^2} \tag{5.8}$$

Thermodynamical properties before and after the rotor are found as done in a similar way in the compressor stage design, using the efficiency. The geometrical parameters such as entrance area, rotor inlet diameter and inlet width are calculated as such:

$$A_2 = \frac{\dot{m}_c R T_{02}}{P_2 C_{2r}}, \quad r_2 = \frac{U_2}{2\pi \cdot rpm}, \quad b_2 = \frac{A_2}{2\pi r_2} \tag{5.9}$$

And for the outlet geometries:

$$A_3 = \frac{\dot{m}_c R T_3}{P_3 C_3}, \quad r_{3h} = 0.25 \cdot r_2, \quad r_{3t} = \sqrt{\frac{A_3}{\pi} - r_{3h}^2}, \quad b_3 = b_2 \tag{5.10}$$

Since the flow exits completely axial, there is no need to calculate α_3, $\beta_3$instad is defined as:

$$\beta_3 = \tan^{-1}\frac{U_3}{C_3} \tag{5.11}$$

Knowing all the angles, we obtain the velocities and Mach number at the exit.

$$U_3 = \pi(r_{3h} + r_{3t}) \cdot rpm, \quad W_3 = U_3 \cdot \csc\beta_3, \quad M_3 = \frac{C_3}{k \cdot R \cdot T_3} \tag{5.12}$$

Down here in Table 5.4-5-6and Figure 5.5Figure 5.5 we present the results obtained after this procedure and the velocity triangle at entrance and exit of the rotor.

Table 5.4: Geometrical Data HP turbine

Geometrical Data			
Rotor Inlet		**Rotor outlet**	
A_2[m]	0.0015	**A_3 [m^2]**	0.0016
d_2[cm]	10.41	**R_{3h} [cm]**	1.3
B_2[mm]	4.5	**R_{3t} [cm]**	2.58
α_2 [°]	75.04	**β_3 [mm]**	4.5
β_2 [°]	29.92	**α_3 [°]**	0
		β_3 [°]	46.83

Table 5.5: Velocity Data HP turbine

Velocity Data			
Rotor Inlet		**Rotor outlet**	
C_{2r} [m/s]	120.35	**C_{3a} [m/s]**	150.44
C_{2u}[m/s]	372.51	**C_{3u} [m/s]**	0
C_2 [m/s]	391.47	**C_3 [m/s]**	150.44
U_2 [m/s]	429.82	**U_3 [m/s]**	160.36
W_2 [m/s]	133.30	**W_3 [m/s]**	219.88
M_2 []	0.53	**M_3 []**	0.21

Table 5.6: Thermodynamical Data HP turbine

Thermodynamical Data			
Rotor Inlet		**Rotor outlet**	
T_2 [K]	1449	**T_3 [K]**	1365.4
P_2 [Pa]	663200	**P_3 [Pa]**	470390
ρ_2 [kg/m^3]	1.7427	**ρ_3 [kg/m^3]**	1.145

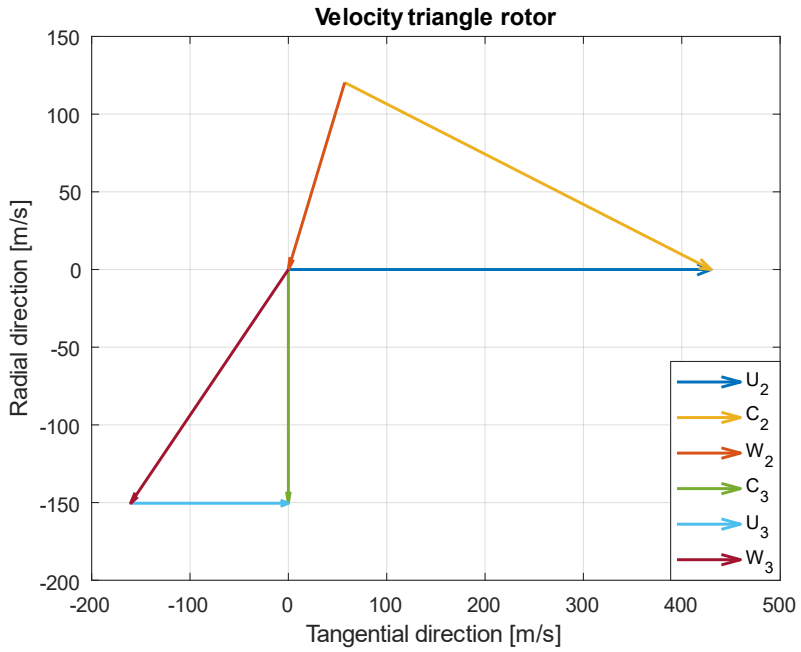

Figure 5.5: Velocity triangles HP rotor

It must be said that we have decided to opt for straight radial blades, but knowing the relative angle β_2, the incidence angle *i* and the deviation angle δ_3 at the exit, the blades angles could be calculated. In this way the flow is better channelled, we could have lower losses and therefore higher efficiencies.

5.3.2 Stator Vanes

Regarding the nozzle/stator geometrical design, most of the works found in literature, presents a CFD based design. Aungier in [11] tries a different approach and puts two major constraints:

- Inlet to outlet nozzle radius ratio $1.1 < \frac{r_1}{r_2} < 1.7$
- Number of stator blades < 30
- Blade angle with respect to the tangent $\beta > 5°$

After defining a vaneless space between rotor and stator, whose radius is 1.05 times the inlet diameter of the rotor, we follow those constraints opting for a radius ratio of 1.3 and 19 blades and obtaining the following results:

- Diameter of the machine $D_1 = 13.67\ cm$
- Interpalar distance at stator exit $S = 1.81\ cm$

5.4 Low-pressure Turbine

The same process has been followed for the design and geometrical dimension estimation of the low-pressure stage of the turbine. The initial assumptions are different and this time we know the temperature at the exit of the turbomachine. Therefore, we can calculate directly the enthalpy drop without having to know the power requested by the compressor.

Here we report the initial data and hypothesis:

- 60000 rpm
- Total inlet Temperature T_{01}= 1373.3 K
- Total inlet Temperature T_{01}= 942.04 K
- Total inlet Pressure P_{01}=474770 Pa
- Flow density ρ= 1.147 Kg/m^3
- Mass flow rate $\dot{m}$=0.2695 Kg/s
- Flow coefficient $\Phi = 0.35$
- Rotor meridional velocity ratio $\xi = 1$
- $\frac{r_{3h}}{r_2} = 0.25$
- $\eta_{tt} = 0.88$
- Number of rotor blades n=17
- Number of stator blades Nn= 21

5.4.1 Results

Main results for geometry, speeds and thermodynamical properties, as well as velocity triangles are stated here in table 5.7-5.9 and Figure 5.6.

Table 5.7: Geometrical Data LP turbine

Geometrical Data			
Rotor Inlet		**Rotor outlet**	
A_2[m]	0.0018	**A_3 [m^2]**	0.0051
d_2[cm]	24.74	**R_{3h} [cm]**	3.09
B_2[mm]	2.4	**R_{3t} [cm]**	5.09
α_2 [°]	75.96	**β_3 [mm]**	2.4
β_2 [°]	28.07	**α_3 [°]**	0
		β_3 [°]	43.37

Table 5.8: Velocity Data LP turbine

Velocity Data			
Rotor Inlet		**Rotor outlet**	
C_{2r} [m/s]	217.65	**C_{3a} [m/s]**	272.07
C_{2u}[m/s]	685.88	**C_{3u} [m/s]**	0
C_2 [m/s]	719.59	**C_3 [m/s]**	272.07
U_2 [m/s]	777.33	**U_3 [m/s]**	256.98
W_2 [m/s]	236.09	**W_3 [m/s]**	374.25
M_2 []	1.07	**M_3 []**	0.46

Table 5.9: Thermodynamical Data LP turbine

Thermodynamical Data			
Rotor Inlet		**Rotor outlet**	
T_2 [K]	1188.5	**T_3 [K]**	915.62
P_2 [Pa]	242230	**P_3 [Pa]**	53248
ρ_2 [kg/m^3]	1.149	**ρ_3 [kg/m^3]**	0.1933

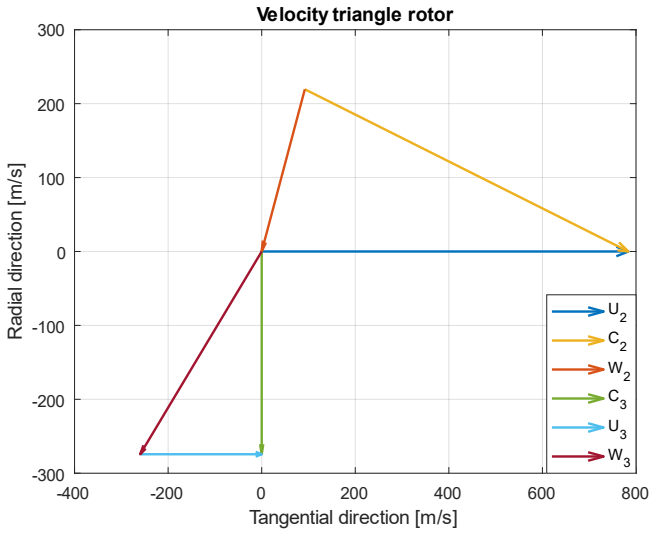

Figure 5.6: Velocity triangles LP rotor

As previously, here are reported the results for the Stator ring geometry.

Table 5.10: Nozzle data LP turbine

Nozzle Data	
D1 [cm]	28.19
S [cm]	3.89

As can be seen the second stage is bigger than the first one because it completes the enthalpy drop and provides the power for both compressor and electric generator. It is more than 2 times bigger than the high pressure one and it produces a net power of 162.85 kW that transforms to a net power available for the generator taking into account mechanical efficiencies of about 122 kW.

Comparing turbines and compressors we can see that High Pressure ones have smaller diameters and dimensions that are comparable. Low pressure turbomachines instead as expected differs a lot because the turbine has to drive the generator.

A partial solution to this difference that could cause geometrical and fitting problems, is to use two electrical generators, one for each shaft. In this way we could split the enthalpy drop in equal parts for the two turbines, hence having a bigger HP turbine but a smaller LP turbine.

With some fast calculation this option has been carried out showing that the rotor of the first stage would be about 4 cm bigger (around 14cm), instead the rotor of the second stage results to be 6 cm smaller (about 19 cm).

The main problem of this configuration is the higher weight and space required to place the second generator, and the fact that you have to synchronize the current outputs at the exit, adding more losses.
For these reasons this option has been discarded.

5.5 Material Selection

Choosing the material for a turbine is not as simple as it might seems. The gasses entering the first stage in our case have a temperature around 1503 K high enough to melt most of normal materials or to lower down their mechanical properties sufficiently to prevent us from using them because they can't withstand the high stresses to which they are subjected.
On one hand, we've deliberately chosen a total inlet temperature (TIT) this high to take the most advantage from the fuel and to complete the combustion in order to have lower emission and lower SFC. On the other hand, we don't want to use techniques to cool the blades as done in most of the aeronautical engine today, because our rotor is really small and holes or channels to pass a cold flow would be difficult to manufacture and could lead to mechanical weakening. Furthermore, it will reduce the mass flow entering in the engine. This are the main reason why blade/rotor cooling is not used in radial turbines.
The main features that a material must have to be a suitable candidate for radial turbine usage are:

- High temperature resistance
- Creep resistance
- Fatigue resistance
- Corrosion and oxidation resistance
- Small thermal expansion coefficient
- Impact and shock resistance
- Low density
- Good machinability

All these features are difficult to be found in a unique material, and the engine manufacturers usually use alloys. In this case Nickel superalloys are the most appropriate for the high temperature and corrosive environment. As today, engine

manufacturer like General Electric and Rolls-Royce uses various types of alloys based on nickel for their turbine blades: Rene, CSMX, Inconel and Waspalloy. This are usually coated with rare earth such as Molybdenum, Chromium, Niobium and Yttrium, to avoid corrosion and are cooled down by mean of an air flow passing inside of the blade. This allows for smaller temperature gradients and reduces deformations.

In the last 40 years two materials have been found to be suitable for high temperature applications: Silicon Carbide (SiC) and Silicon Nitride (Si3N4). The second one presents good mechanical properties that remain stable at elevated temperatures well above our peak temperature of 1500 K. Based on the method of manufacturing of these particular alloys (Reaction bonded, sintering, Hot isostatic pressing) there is a slightly variation of their properties, with major corrosion resistance or higher mechanical resistance improvement. We report in

Figure *5.7* thermophysical and mechanical properties of this advanced ceramics materials.

Materiale	SiC	RBSN[1]	HPSN[2]	SSN[3]
Densità (g/cm^3)	3.11	2.5	3.2	3.1
Modulo di Weibull m	12	15	10÷20	4÷10
Carico di rottura a flessione a 25°C (Mpa) a 1000°C	500 475	296 300	800 450	880 510
Rapporto di Poisson	0.27	0.24	0.27	–
Modulo elastico E (Gpa) a 25°C	380	175	316	250
Calore specifico c ($J\ kg^{-1}\ k^{-1}$)	–	700÷1100	800	900
Dilatazione termica α (10^{-6}/°C) tra 500÷1000°C	3.8	3.2	3.6	4.0
Conducibilità termica ($W\ m^{-1}\ k^{-1}$)	9÷100	12	18÷35	15
Tenacità a frattura k_{IC} ($MPa\sqrt{m}$)	2.4	3.6	5.3	7.0
Resistenza agli shock termici (in acqua) DT(°C)	370	440÷600	570	900

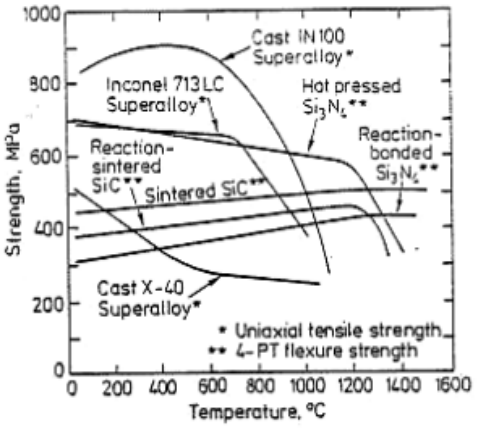

Figure 5.7: table with Ceramic material properties, and subsequent temperature strength graph; (RB= reaction bonded, HP= hot isostatic pressing, S=sintering)

As can be seen Si_3N_4 and SiC presents higher strength over 1200°C in respect to Nickel based superalloys currently used in aeronautics. Corrosion resistance is assured for this material, the only problem are impact resistance and brittleness. In

aeronautics these are a major concerns, because if the turbine breaks the engine stops working and the plane falls from the sky. It is also the main reason for the little use of this material as today.

NASA and other researchers to solve this problem introduced and developed Ceramic Matrix Composites (CMC). These materials have a core of one of the alloys listed before, but they are reinforced with carbon fiber or other high shock resistance material.

In reference [12] a 100kW automotive gas turbine engine was developed, with a TIT of 1350°C (1623 K) was tested using a small turbine made of monolithic ceramic material or by CMC with different kinds of reinforcements such as fibers, particle and wiskers. The turbine used has dimensions similar to our high-pressure stage.

The aforementioned engine undergoes several tests at the highest temperature, showing that this composite material can overcome all the problems of the ceramic ones such as particle impact, and hot corrosion even providing a better strength and creep resistance Figure 5.8.

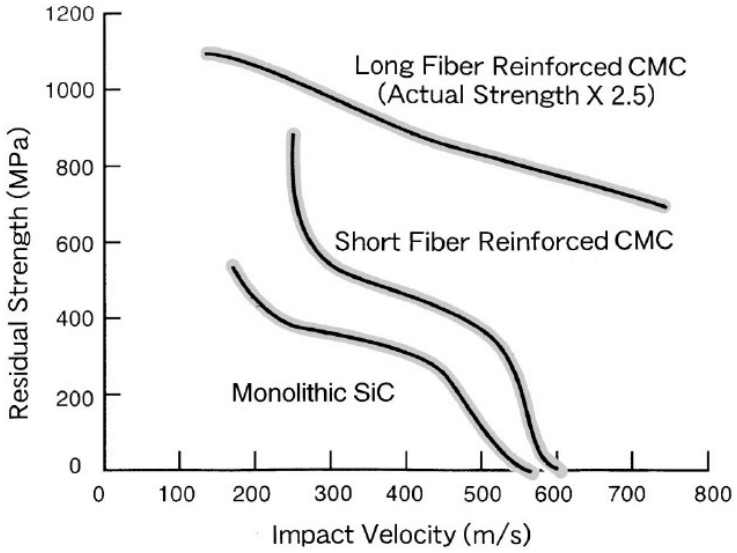

Figure 5.8: Strength variation with temperature for ceramics materials

Therefore, for our high-pressure turbine this material will be used ensuring high reliability, shock and fatigue resistance.

The only thing that needs to be considered is the manufacturing: we want to avoid defects that could cause poor mechanical characteristics. Therefore, if sintering or

3D printing is used, raw material needs to have the best quality. Inevitably, the costs will go up, but they could be balanced by raising the turbine inlet temperature.

The LP-turbine undergoes fewer stresses and lower temperature, allowing us to use Nickel based superalloys, that have been tested and used in the past 20 years allowing us to have a reliable and consistent stage, easier to be manufactured without defects or inclusions.

6 Shaft design

Once designed the turbomachinery we proceed with the design of both the shafts used in our engine, to have an idea of the dimensions, weight of a shaft capable to withstand high rotational speeds and moment generated from the turbomachines. A shaft is a rotating member, in our case of circular cross section that is used to transmit power and motion.

Since we are trying to build a low weight and compact engine, we will try to make the shaft as small as possible. Having decided to use two parallel shaft means that we can decide to reduce as much as possible the dimensions of one of them, because combustion chamber and recuperator will be placed around the other one. Basically, we will have LP compressor and turbine near each other with a small shaft in between, the HP one instead will be longer.

6.1 Material selection

The first step of shaft design is the choice of the material. There are few important properties that a material needs to meet to be eligible for use in a gas engine. The high rotational speed requires greater strength, and capacity to withstand applied loads, good elastic modulus, fatigue resistance, corrosion resistance, but also good machinability. Usually low-medium content carbon steels are used, alloyed with nickel chromium, or vanadium, to avoid oxidation and corrosion.

As we can see from Figure 6.1: Low carbon steels material properties, their Yield strength varies between 200 and 600 MPa thanks to the presence of carbonium.

Other materials such as titanium alloys (grade 5 and 6) could be used in case high strength are required, but stainless steels should be good enough for our purposes and looking at costs seen that titanium is expansive to buy and manufacture, we will be able to significantly cut them using steel.

For both shafts the choice fell on C40 carbon steel or its equivalent AISI 1040.

Material	Ultimate tensile strength, N/mm^2	Yield strength, N/mm^2
Plain carbon steels		
$C\,07$	320 – 400	200
$C\,10$	340 – 420	210
$C\,15$	370 – 490	240
$C\,20$	440 – 520	260
$C\,25$	460 – 550	280
$C\,30$	500 – 600	300
$C\,40$	580 – 680	330
$C\,45$	600 – 750	380
$C\,50$	660 – 780	380
$40\,Ni\,3$	750 – 1050	600
$30\,Ni4\,Cr_1$	1000 – 1150	600
$40\,Cr\,3\,Mo1\,V20$	1350	1120
$40\,Cr_1$	700 – 850	540

Figure 6.1: Low carbon steels material properties

6.2 High-pressure shaft

Since the engine will work always at the same rotational speed, we can assume that loads applied to the shaft will be static. The high-pressure shaft is evaluated as if it is subject only to torsional loads because bearings (that acts as constraints) will be placed near the turbomachines cancelling bending moments.

In reference [13] a relationship for the diameter of the beam in function of torsional moment and maximum shear stress is found:

$$d^3 = \frac{16}{\pi} \cdot \frac{M_t}{\tau_{max}} \tag{6.1}$$

$$with\ M_t = \frac{Power\ \cdot 60}{2\pi \cdot rpm}, \quad \tau_{max} = \frac{\sigma_s}{2 \cdot \mathrm{sf}} \tag{6.2}$$

Using AISI 1040 and an high safety factor (sf=5) to avoid problems and to count forces/moments that we did not predict we obtain the following results:

- Shaft diameter d=0.010 m
- Torque moment $M_t = 6.03$ Nm

As we can see, the diameter seems to be really small but in line with the other dimensions of the high-pressure components, therefore to avoid problems like buckling it needs to be as short as possible.

6.3 Low-pressure shaft

For this shaft we will be considering also bending moments, because of the high-speed electric generator attached to the shaft. Assuming the weight of the generator to be around 10kg at a distance of 0.2m from the nearest bearing (constraint) we can write:

$$M_{b\_max} = F \cdot l = \ 20\ Nm \tag{6.3}$$

The torsional moment is calculated as before paying attention to use the right rpm (60000) and power.

In the case of bending and torsion happening together, the formula to obtain the diameter is slightly different:

$$d^3 = \frac{16}{\pi} \cdot \frac{M_{t_e}}{\tau_{max}} \quad \rightarrow$$
$$with\ \ M_{t\_e} = \sqrt{{M_t}^2 + {M_b}^2} \quad equivalent\ twisting\ moment \tag{6.4}$$

Or

$$d^3 = \frac{16}{\pi} \cdot \frac{M_{b_e}}{\tau_{max}} \quad \rightarrow$$
$$with\ \ M_{b_e} = \frac{1}{2} \cdot \left[M_b + \sqrt{{M_t}^2 + {M_b}^2}\right]\ \ equivalent\ \ bending\ moment \tag{6.5}$$

The two results obtained using a safety factor of 3 are a bit different, 1. 38 cm using the equivalent twisting moment, and 1.62 cm with the equivalent bending moment. The bigger one will be used to maintain a conservative margin, and because currently on the market, the nearest diameter dimension is 0.016 m.

6.4 Final considerations

To support the rotational components of the engine both axially and radially hence improving shaft stability, bearings are placed near the coldest part of the

turbomachine (before the compressor and after the turbine), to avoid misfunctioning. Roller and ball bearings are used. A structural analysis should be performed to decide the correct positions.

This is just a preliminar analysis to give an estimate of the dimensions of the shaft that will allow us to calculate weight and overall dimensions, and it can't be considered satisfactory. Before confirming this, a finite element analysis should be carried out, with a focus on natural frequencies estimation to avoid resonance problems.

7 Combustion chamber design

Combustion chamber is a crucial piece of a gas turbine engine, in here fuel is added and through an igniter the combustion is fired generating, through an exothermic chemical reaction, huge quantities of heat that brings fluid temperature up of hundreds of degrees, providing to the airflow the energy necessary to drive the turbine. It is usually situated between compressor and turbine (in our case ahead of the entrance the flow passes through the recuperator) and delivers to the high-pressure turbine a gas flow at high velocity and temperature.

We want to design the best combustor for our applications, and to do so we need to satisfy a lot of requirements that are going to limit our freedom of design. Starting with a high efficiency combustion, we want to have as low-pressure losses as possible, a small fuel consumption, low pollutants emissions, high maximum temperature, complete combustion, but also ability to use the different kinds of fuel purposed, minimum costs and maintenance.

The first step is to select the chamber architecture between the most used nowadays:

- *Tubular*: made by one or more cylindrical chambers fitted radially around the shaft each one with its own stream, flame tube and air chasing. They are interconnected to uniform pressure, temperature e to spread the flame Good efficiency and ease to reparir but heavy and with high pressure loss
- *Annular*: it's the most used in today's engines. The flame tube is restrained between and internal and external chasing. It is smaller, lighter, and more efficient than the first one, but it is not reparable.
- *Tubo-annular*: it is a mix of the first two configurations, with an external liner in common for all the chambers.

Another parameter to choose is whether we want the flow to enter the chamber directly or from the end of the chamber (Reverse flow).

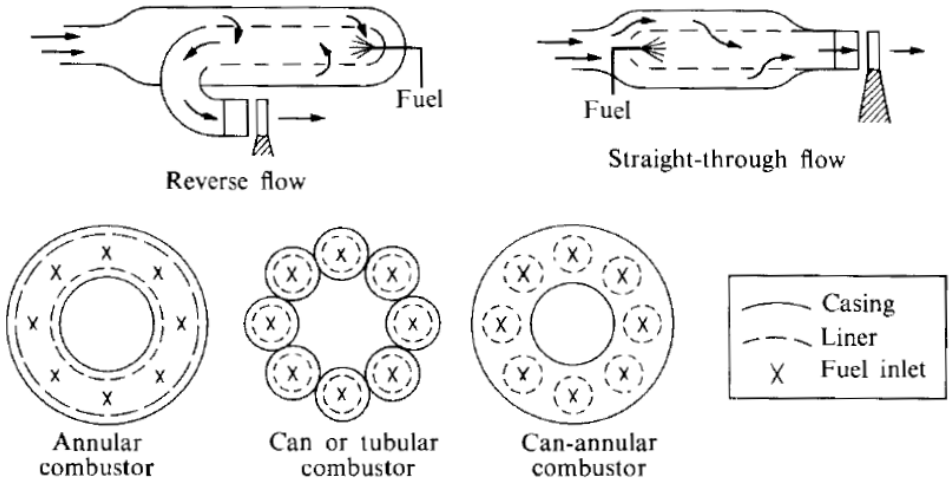

Figure 7.1: types of combustion chambers [14]

After some considerations, and looking at other microturbines available on the market, an annular reverse flow combustion chamber has been chosen because it allows for lower pressure losses, smaller dimensions and therefore shorter shaft and overall configuration, that in a light aircraft is fundamental. The reverse flow permits a smaller frontal area and consent a better overall positioning of the recuperator.

7.1 Geometry and Working principle

As can be seen in Figure 7.2, a combustion chamber is composed by an elevated number of parts. The air flow exiting from the recuperator enters the chamber through a diffuser that reduces it's velocity to a suitable one in order to have the best combustion speed and to avoid the flame blow-off. (if the speed is too high or slow the combustion stops)

A swirler is put at the entrance to create recirculation areas where the flow is turbulent and the fuel that enters from the nozzle (simple, duplex…) is better mixed with the air. An igniter similar to automotive candles, unleash the spark and starts the combustion. The chemical reaction take place inside the liner, that can be divided in 3 areas:

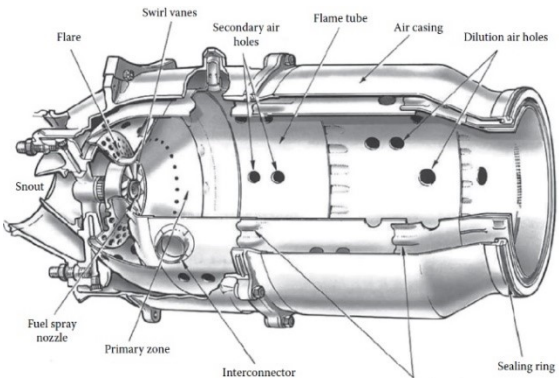

Figure 7.2: combustion chamber geometry

- *Primary zone:* where the complete combustion of the blend happens
- *Secondary zone:* where there is an input of clean air to bring temperature down and complete the combustion if there is any excess of fuel
- *Dilution zone:* where the last part of air enters, to allow a further lowering of the temperature to make it acceptable to enter the turbine.

With these three zones we manage to have a complete combustion of all the hydrocarbons thus reducing the emissions of NOx and CO_2 that is feasible only in a short range of temperature (Figure 7.3), higher than the one tolerable by the turbine.

The eventual problem will be to find the right materials and cooling techniques to avoid the melting and reduction of mechanical properties.

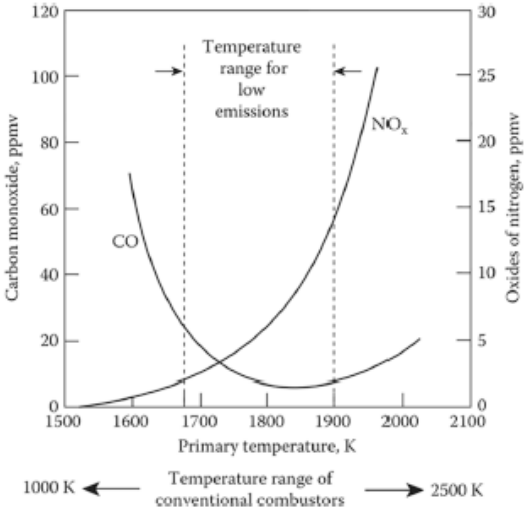

Figure 7.3: pollutants emission in function of temperature [17]

In the next paragraph based on all the things seen so far, a dimensional design will be carried on, and dilution rates will be decided.

7.2 Dimensional Design

In a real combustor one of the most important things to keep under control is the ratio between the fuel mass rate and the quantity of air that arrives from the compressor, because a higher quantity of air makes the mixture too lean to be flammable, but a richer mixture generates unburnt species and raise pollutant emissions. In aeronautics for this reasons it is necessary to assure that the combustion reaches values that are almost stoichiometric, and that the percentage of fuel in the mixture stays between the inflammable limits of the fuel, that in our specific case (Methane) are 4.4% to 17% with the first one that represent the lover limit value, instead the latter represent the explosion limit of the mixture.

The equivalence ratio is defined to understand if a combustion is stoichiometric or not as:

$$\varphi = \frac{\mathrm{f}}{\mathrm{f_{st}}} = \frac{0.0244}{0.0581} = 0.42 \tag{7.1}$$

With f being the ratio between fuel flow rate and air flow rate, and f_{st} the same but in stoichiometric values. From the value of φ we can understand that our mixture is far from being stoichiometric, it is lean and even outside of the flammable limit of methane. For this reason, the airflow entering the combustor will be divided between the three zones, to have the best combustion possible. The lower flammable limit is around φ=0.75 but in order to have a near stoichiometric reaction an equivalence ratio of 0.9 will be used. Therefore, the percentage of air to enter the primary zone will be calculated as such:

$$\dot{\mathrm{m}}_{\mathrm{primary\_zone}} = \frac{\dot{\mathrm{m}}_{\mathrm{f}}}{\varphi \cdot \mathrm{f_{st}}} = 0.1228\ \mathrm{kg/s} \tag{7.2}$$

With the obtained result we can affirm that the 46.67% of the flow coming from the compressor directly enters the combustion chamber. To calculate the other two air flows for the secondary and dilution zone we have to define how big will be the cooling flow. To do so, the cooling effectiveness is determined as:

$$\Phi = \frac{T_g - T_m}{T_g - T_c} = 0.33 \tag{7.3}$$

Where T_g is the primary zone gas temperature, T_m is the average metal temperature (we can use the exit temperature of the combustion chamber) and T_c is the cooling air temperature that we take equal to the Temperature of the air entering the combustion chamber.

We want T_g to be between 1700 K and 1900 K because as we can see in Figure 7.4, this is the range to have minimum pollutants emissions and a good and complete reaction. This is not easy to obtain because in stoichiometric conditions the flame temperature of methane reaches, at ambient pressure, temperatures over 2100 K, temperature that gets higher with the high pressure in the combustion chamber. We choose a value for T_g of about 1800 K, with this estimate if we decide to proceed

with a film cooling, an airflow of $\dot{m}_{cooling} = 0.021 kg/s$ (8%) is obtained from the graph in Figure 7.5.

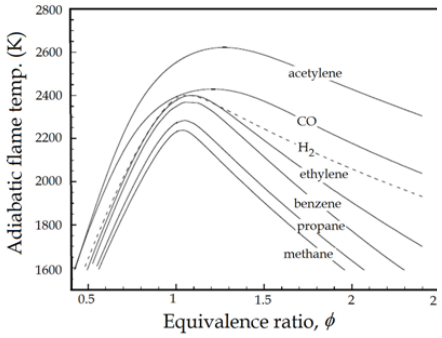

Figure 7.4: Flame temperature vs eq. ratio

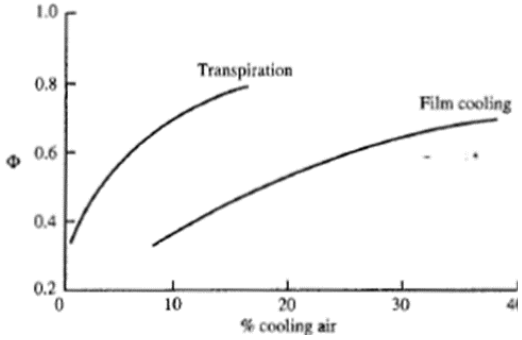

Figure 7.5: percentage of cooling air vs eq. ratio [14]

Therefore, an airflow of 0.1192 kg/s (45.33%) remains to be divided between primary and dilution zones, to cool down the flow and complete the combustion. Most of that will go into the dilution zone.

Having divided the airflow, we proceed to calculate the actual dimension of the combustor using empirical formulae developed by Sawyers [15] and Lefebvre [16], as found in reference [17]. We begin calculating the frontal area (complete with casing) knowing as suggested by Sawyers that the liner area is about 0.6-0.7 times the reference one.

$$A_{ref} = \left[R \cdot \left(\frac{\dot{m}_{air}\sqrt{T_3}}{P_3} \right)^2 \left(\frac{\Delta P_{3-4}}{q_{ref}} \right) \left(\frac{P_3}{\Delta P_{3-4}} \right) \right] = 2.13e-3m^2 \qquad (7.4)$$

$$A_{liner} = 0.65 \cdot A_{ref} = 1.386e-3m^2 \qquad (7.5)$$

Where the values of data behind parenthesis are empirical and presented in Table 7.1.

Table 7.1: Pressure losses for various type of combustion chamber

Type of chamber	$\frac{\Delta P_{3-4}}{P_3}$	$\frac{\Delta P_{3-4}}{q_{ref}}$
Tubular	0.07	37
Tuboannular	0.06	28
Annular	0.06	20

Since it is an annular combustor, we decide to put its inner diameter at 3.5 cm thus we can derive the outer diameter from the annulus area formula.
Following those sources, we determine the length of primary, secondary and dilution zone with the following assumptions:

- *Primary Zone* 2/3 or ¾ of total diameter
- *Secondary Zone* ½ liner diameter
- *Dilution Zone* 1.5-1.8 times liner diameter

For the primary zone, the bigger value is used because a longer zone traduces in longer residency values that leads to lower emissions. For the dilution zone an equation was found in literature providing the dimensions in function of liner diameter and a Pattern factor (PF) that seen how we took the values, is basically the cooling effectiveness (Φ) seen before.

$$\frac{L_{DZ}}{D_{liner}} = 3.83 \ - 11.83 \cdot PF \ + \ 13.4 \cdot PF^2 \qquad (7.6)$$

Table 7.2: Dimensions of combustion chamber

Diameter [m]	Primary zone [m]	Secondary zone [m]	Dilution zone [m]	Total length [m]
0.079	0.059	0.038	0.0679	0.165

7.3 Other considerations

Seen that the air flow arrives at the combustion stage after having passed the recuperator and remembering that the air exits the compressor at Mach 0.25 we conclude the flow moves at an adequate velocity and therefore there is no need for a diffuser at the beginning, simplifying the geometry of the chamber. Due to the nature of our engine, that works always at its maximum efficiency and rotates at constant speed, there is no need for a variation of the quantity of fuel entering the combustion chamber, to change the power output. Therefore, fuel nozzle could be made as simple as possible, without a double channel as in the duplex ones. Another way is to incorporate the injectors in the swirler design as done in reference

[17], in this way as the air enters, it is mixed in a turbulent flow improving the combustion.

The residence time of the mixture in the chamber is estimated with the following formula:

$$\tau_{resident} = \frac{\rho_{03} A_{ref} L_{tot}}{\dot{m}_3} = 4.6\, ms \tag{7.7}$$

Another parameter to look at is the ability of the combustion to sustain itself continuously with the variation of parameters such as flow rate and pressure variations, without having the flame blown away or suffocated. To see if our combustion is stable, we calculate the combustion loading parameter and we look at Figure 7.6 which returns us for a phi of 0.9 a stable combustion.

$$CLP = \frac{\dot{m}_3}{P_3^{1.8} \cdot Vol_{comb}} = 1.15 \quad \left[\frac{lbm}{s \cdot ft^3 \cdot atm^{1.8}}\right] \tag{7.8}$$

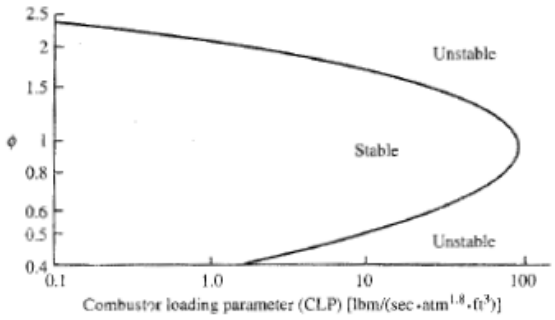

Figure 7.6: combustor loading parameter for a stable combustion

7.4 Material selection

The choice of the material to be used for the liner is a critical one as it changes all the efficiencies of the engine, because the higher the temperature in the combustion chamber the better the thermal efficiency is. Due to the high temperature reached in the engine currently on the market, it is customary to use nickel based superalloys and in general ceramic materials such as Hastelloy X, or Inconel 625/718 due to their high operational temperature (over 1000°C) and their capacity to resist at high thermal stresses, abrupt thermal gradients, fatigue, and high frequency vibrations caused by combustion. Furthermore, the liner is a thin wall

structure that must resist to a corrosive environment and to high differential pressure. Ceramics are the perfect materials to satisfy these requirements.

In our case though, we decided to get to an even higher temperature to maximize efficiencies and power outputs, fundamental for minimizing pollutant emission and taking the best out of a turbogenerator. Our exit temperature is about 1500 K, and the flame temperature is over 2000 K, imposing a change of materials. A way to solve this problem is to use thermal barrier coatings made of advanced ceramic materials. Thermal barrier coatings are widely used to maximize the effects of external cooling air, maintaining metal temperature within creep limits, and helping to mitigate thermal gradients. They are usually made of Silicon carbide, silicon nitride or zirconium dioxide. The latter seems to be the most promising one, seen that it has good mechanical properties at over 2000°C and its structure is maintained at lower temperature when stabilized with Yttria. Our combustion chamber will be made of multiple layers as we can see in Figure 7.7, with a nickel superalloy giving mechanical strength, two substrates to avoid corrosion and to prevent rapid changes in mechanical properties of the material, and a thermal barrier of Yttria stabilized zirconium. In this way we can guarantee all the requested properties at high temperature. Coatings are applied with additive manufacturing techniques like diffusion bonding or spraying.

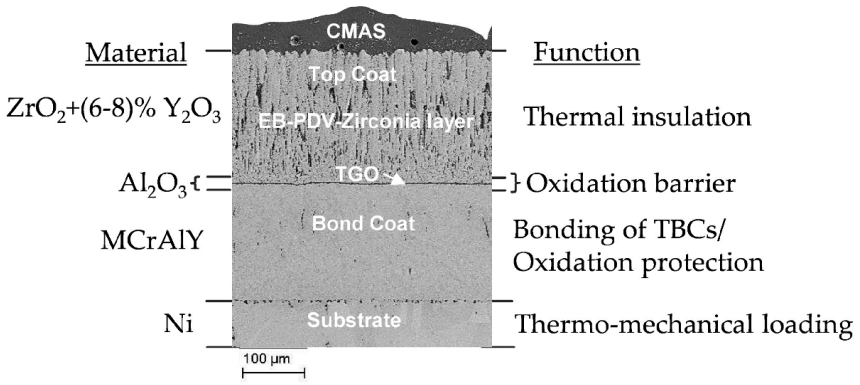

Figure 7.7: Layers of combustion chamber material

7.5 Emissions & fuels

As known emission of pollutants and particulate for a gas turbine engine depends by many things such as temperature, power requested, equivalence ratio and others. Ideally, in a combustion reaction, only water (H_2O) and carbon dioxide (CO_2) are obtained. Those two are not pollutants, but the first, released at high altitude

with temperature below zero, condense creating trails and clouds blocking the sun and preventing the regeneration of ozone. The latter is the major responsible for the greenhouse gasses (GHG), thus contributes to global warming. Not much can be done to reduce the emission of this elements because they are the natural product of combustion, except reducing overall consumptions, that is one of the objectives of this work. However, the real combustion reaction of a hydrocarbons is the one reported here:

$$CH_2 + \frac{3}{2}\cdot(O_2 + 3.76N_2) \rightarrow \alpha_1 CO_2 + \alpha_2 CO + \alpha_3 H_2 + \alpha_4 H + \\ + \alpha_5 H_2O + \alpha_6 OH + \alpha_7 O_2 + \alpha_8 O + \alpha_9 N_2 + \alpha_{10} NO + \alpha_{11} NO_2 \quad (7.9)$$

We can observe that other chemical species are generated, which, even if in small quantities, are pollutants. The biggest problems are caused by Nitrogen oxides (NOx), particulate matter, carbonium oxide (CO) and unburned hydrocarbons (UHC). The production of NOx should be avoided because it contributes to smog production, ozone, acid rain and produces nitrates that alter the environmental equilibrium; carbonium monoxide constitutes a problem for human respiration, and huge quantities are lethal.

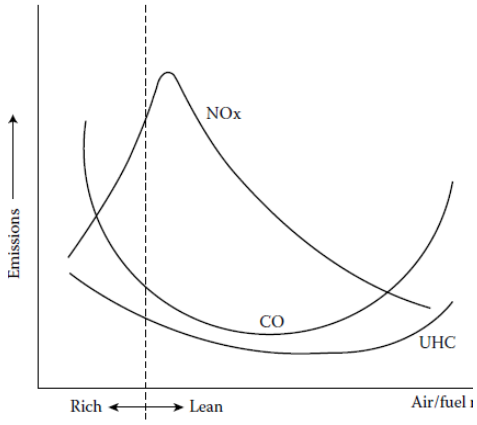

Figure 7.8: Emissions as function of eq. ratio [9]

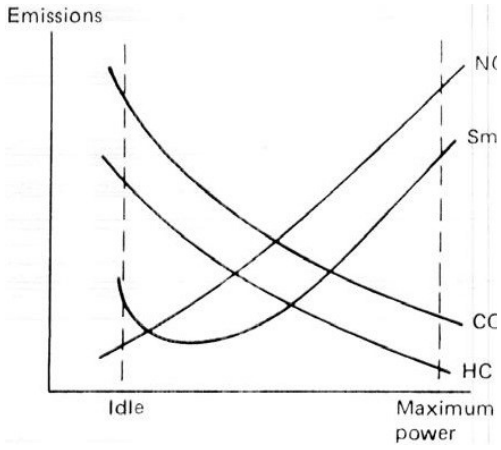

Figure 7.9: Emissions as function of power [16]

The graph reported (Figure 7.4, Figure 7.8, Figure 7.9) shows that the production of this pollutants behaves in an opposite way: to reduce NOx we should have a fast and cold combustion (thus a small power request), this leads to a high emission of CO and UHC caused by an incomplete combustion of the entire fuel. On the other hand, to reduce UHC an CO there should be a high temperature combustion (with

a high power request) and therefore a long residence time in the combustion chamber. To get the lowest emission usually NOx are limited using in the primary zone a lean mixture (between 0.8-0.9) and high temperature in the range between 1700-1900 K to assure the complete burn of hydrocarbons. The lean mixture will make the flame less stable, but with swirler, recirculation zones and flame holders can improve stability and complete combustion.

Another method to reduce emissions and consumption is to use high performance and natural fuels. Nowadays, if a combustion chamber is properly designed, its performance and operating characteristics, are not sensitive of the type of fuel used [9] [18], at least during cruise. We did all the calculations for this engine using methane natural gas as fuel, but other fuels such as Biodiesel, Bioethanol and SAF have been employed to calculate fuel consumption.

We chose these four fuels because differently from Kerosene (JET A-1) commonly used in aircraft, they don't derive from hydrocarbons because they derive from biological sources that are sustainable, with the exception of Natural gas. Some considerations and pros and cons of those fuel are reported here below.

- *Natural Gas (Methane):* this has been chosen to be the main fuel for our engine due to its high energy content with respect to every other fuel, and because it presents lower CO_2 emissions. It is considered a fossil fuel but allows us to have smaller consumption than other fossil and biomass combustible.
- *Biodiesel:* This fuel has been chosen because it is a sulphur free, biodegradable, renewable fuel produced from alcohol, vegetable oil or animal fats that are usually waste products. It is one of the most promising biofuels currently available due to its high heating value and similarity to current diesel. As seen in various research [18] [19], the major advantage of this alternative fuel is the reduction of CO_2 produced. At reference [18], pure biodiesel has been confronted with Kerosene and Natural gas showing a consistent reduction of UHC, CO and CO_2 with respect to kerosene, but also to natural gas at the same power output. The NOx production is on the contrary a little bit higher but comparable. Seen the calorific value similar to Jet A-1 this fuel looks like one of the best options to be used.

- *Bioethanol:* Is the fuel with the lowest calorific value between the chosen ones. This comports a higher consumption, and therefore higher emission of CO_2 for the same amount of energy output [20]. It is produced from agricultural feedstocks, corns and sugarcane so the native material counterbalance the carbon dioxide produced during combustion making it almost a net-zero carbon emission fuel. In [20] a comparison between natural gas, diesel and bioethanol was done showing that it can produce up to 90% less NOx and similar emissions of CO_2 and H_2O, but the higher quantities of fuel requested for the same use makes it less desirable to be used.
- *Sustainable Aviation Fuel (SAF)*: Is a fuel chemically similar to Jet A-1, and it is currently used blended with kerosene in some flights because it can be used in normal jet engines without any modifications. It was developed with the aim to reach net-zero emissions by 2050, it reduces carbon dioxide emissions up to 80%. It is produced as the others by agricultural feedstocks and waste oils [21]. The other emission of pollutants remains almost unchanged, with a slightly lower production of NOx and SOx depending by the raw material used, and the lower flame temperature reached.

To conclude, all of these fuels are a good alternative to power our light aircraft because they reduce pollutants emitted at every flight. With the evolution of materials and CFD a lot more can be done in order to improve consumes and emissions.

8 Heat exchangers design

An heat exchanger is a piece of device used to transfer heat between two fluids using a combination of convection and conduction, that can be employed both in cooling and heating processes. It is made by a high thermal conductivity material and can have different setups. At first, they can be classified based on the relative motion between the fluids: *parallel-flow* when the fluids enter from the same direction, *counter-flow* when fluids enter from opposite direction and *cross-flow* when fluids are perpendicular to one another.

For our application we are interested in compact heat exchangers therefore we can divide them into two types:

- *Shell and tube*: they are the simplest of the devices, made of tubes inside of which one of the fluids flows, surrounded by a shell where the other is introduced. There can be several variations of this type of exchanger mostly with a different path of the inner tubes. In order to increase the exchange area, fins can be introduced around the tubes, also helping creating turbulence and slowing the fluid down.
- *Plate*: these types of devices are amongst the most compact ones; they are made of lots of plates stacked together. Between the plates channels are formed where one fluid can pass and be cooled down by the other fluid on the adjacent channels. Even in this kind of devices fins or wavy surfaces can be introduced to improve the exchange area and make the exchanger more compact.

In chapter 3 we have introduced the two heat exchangers used in our engine, intercooler and recuperator, described how they work and where they are placed in the cycle. In the next paragraph we are going to decide which type is the best to use for aircraft lightweight application and dimension them.

8.1 Intercooler

Starting with the intercooler we have seen that it is an air-to-air exchanger that uses outside air to cool down the fluid after the first compressor, in order to have smaller dimensions of the compression stages and higher net power available to our engine due to the small one requested to spin the compressors. This type of heat exchangers are mostly used in automotive application and in turbocharged engine. In aeronautics there are few aircraft using them, one of the most famous is the P-51 Mustang, but some new prototypes are being developed to adapt this device in turbofans.

To have the best efficiency and the lowest dimensions we have decided to use a cross flow exchanger as most of the intercooler available on the market and a plate triangular finned shaped intercooler. This design is heavier than a straight tubular configuration but allows for a bigger exchange area thus reducing the overall weight. We based our design on a similar one found in reference [22]. The main design requirement is a 60% effectiveness, in a compact and low weight layout. To find the correct and necessary heat exchange area the NTU (Number of transfer Units) method is used. This allows to find the rate of heat transfer knowing the effectiveness and the quantity of heat to be exchanged. We used the following equations:

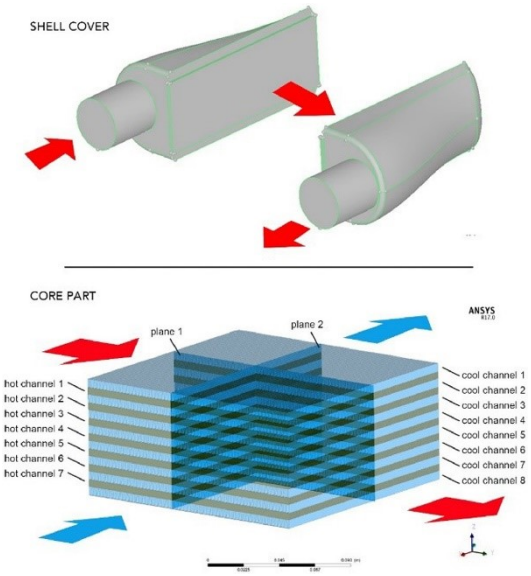

Figure 8.1: intercooler design

$$NTU = \frac{\ln\left(\frac{1-\varepsilon}{1-Cr\cdot\varepsilon}\right)}{1-Cr} = 1.124 \tag{8.1}$$

$$A_{scambio} = \frac{C_{min}\cdot NTU}{U} = 2{,}0m^2 \tag{8.2}$$

Where C_{min} is the minimum between the products of mass flow rate and specific heat of the two gasses, C_r is the ratio between C_{min} an C_{max} and U is called heat transfer coefficient that usually varies in the range of 100-500 W/m^{2}K. We supposed it to be 150 W/m^{2}K, because similar values were used in other heat exchangers with similar initial hypothesis.

The material we choose for the element is aluminium because it is lightweight and easy to be formed. Dependently from which alloy we chose it can work at temperatures higher than 600 K becoming a suitable candidate for our exchanger. Seen its density of 2700 kg/m^3 and with the hypothesis of 1mm thickness for the exchange walls de total weight can be derived as follows:

$$M_{ic} = A_{exchange} \cdot h \cdot \rho_{all} + 5 \quad = 10.39\ kg$$
$$with\ \ h = thickness \tag{8.3}$$

Where we added 5 kg to account for tubes ducts and housing of the intercooler.

Seen that we use triangular fins like in Figure 8.2, it is easy to calculate the overall dimensions. Every channel would be 4mm large ($2a_t$) and 6 mm heigh (b_t) for a total of 15 squared layers of 18 cm per side (W=L) stacked one over the other in order to create the channels.

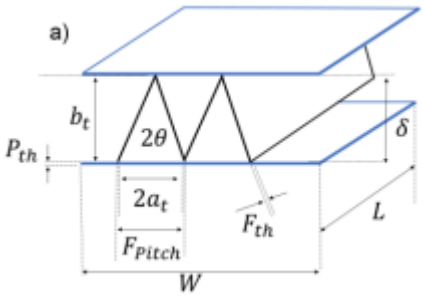

Figure 8.2: geometrical config. intercooler fins

A second setup for the intercooler was considered, in order to produce a high efficiency heat exchanger. Looking at the P-51 Mustang the radiator was an air-to-liquid element placed outside of the body of the aircraft. The idea was to use an air-to liquid intercooler inside the engine, similar to the air-to-air presented before, with the fluid that would be taken behind the fans where another heat exchanger was placed. In this way the fluid could be cooled down by the air flow passing the fans. This hypothesis is a bit complicated but should allow for a more efficient cooling. It was rejected due to the two exchangers needed, a possible problem for a light aircraft such ours, and the fact that a radiator behind a fan could ruin the thrust providing and important amount of drag.

8.2 Recuperator

The recuperator as seen is fundamental to improve fuel consumption ant it is always used for energy production in ground applications since the weight is not a problem and neither are the dimensions. In aeronautics this is almost never used, due to the poor efficiency reachable with a low volume. With the introduction of new advanced materials this element has become possible to be used.

Since high efficiency recuperators are complicated to develop and design, we decided to use the recuperator used by Capstone in its gas turbines C30 and C65, optimized in reference [23]. In this paper the basic recuperator that is a counter flow annular heat exchanger is studied and modified to be mounted on a 300 kW engine, with pressure drops lower than 5%. Down here design and main parameters are reported.

Table 8.1: Parameters of optimized Capstone recuperator [23]

Performance	Original data	Optimal results
n_t	127	182
n_e	195	153
W_h, mm	1.1	1.2
W_c, mm	0.54	0.5
h, mm	2.31	3.0
P, mm	1.84	1.9
B, mm	167	183
C, mm	234	346
C/B	1.4	1.89
D_i, mm	300	300
D_o, mm	626	728
$d_{e,h}$, $d_{e,c}$, mm	1.74/0.98	1.97/0.96
$Re_{h,ch}$, $Re_{c,ch}$	740/706	530/506
h_h, h_c,W/(m^{2}K)	303/483	186/353
K, W/(m^{2}K)	186	121
ΔT_m, K	53.94	53.94
ε, %	85.3	85.3
A_h, m^2	49.89	76.28
Q, $\times 10^3$W	500	500
W_t, kg	60	92
δP_h, %	6.80	3.42
δP_c, %	1.94	1.67
δP_{tot}, %	8.74	5.09

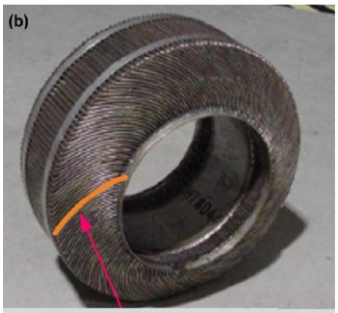

Involute-profile heat exchange element

Figure 8.3: Recuperator design

Operating parameters of recuperator in 300 kW power-level microturbine.

Parameters	Gas side	Air side
Mass flow rate, kg/s	1.805	1.727
Inlet temperature, K	887	581
Outlet temperature, K	645	842
Inlet pressure, $\times 10^3$Pa	112	820

We can see that the 300kW-engine weights 92 kg and has a mass flow rate entering of 1.7kg/s for a 76m^2 heat exchange area.

We know that the weight of a recuperator varies linearly with the density of the material of which is composed, the entrance mass flow rate and the efficiency (or in our case the NTU that can be easily determined), thus we can write the following relation:

$$M_{ceramic} = \frac{\rho_{ceramic}}{\rho_{stainless}} \cdot \frac{\dot{m}}{\dot{m}_{rif}} \cdot \frac{NTU_{ceramic}}{NTU_{rif}} \cdot M_{rif} \quad (8.4)$$

Seen the elevated temperature to which the material undergoes because of the gasses exiting the turbine, the material can't be stainless steel as per the capstone prototype, but we can change it to Silicon nitride (Si_3N_4) as we have seen that it can reach temperatures higher than 1200 °C. This material not only has a great high temperature mechanical resistance and thermal conductivity, but it is also a light material with respect to steel (3300 kg/m^3 versus 8030kg/m^3 of steel) and allows for additive manufacturing production techniques.

Using also the equation 8.1 and 8.2 we manage to determine all the parameters we need:

- Exchange Area: A_e=10.94 m^2
- Weight: $M_{ceramic}$= 7.87 kg (to which we will add few kg for housing and tubes)
- Overall diameter D_0= 13.72 cm (linear comparison with the diameter of the capstone one)

8.3 Final consideration on heat exchangers

Summing the two weights of the heat exchangers we arrive just higher than 20kg, which for the impact these two devices have on the entire cycle is more than acceptable seen the huge quantity of fuel saved and therefore pollutant emissions not produced. They are a fundamental part that needs to be studied, developed and implemented in every aircraft engine seen the great improvements they could give.

9 Air intake and Exhaust nozzle

At the entrance and exit of all gas turbine engines are placed two ducts with the aim to slow the flow down before the compressor (diffuser) or accelerate the exhaust gas to generate thrust (nozzle). In this chapter we are going to briefly design and dimension these two pieces for our aircraft. Both can be studied by means of one-dimensional gas dynamic equations with the main hypothesis of isentropic flow.

9.1 Air intake

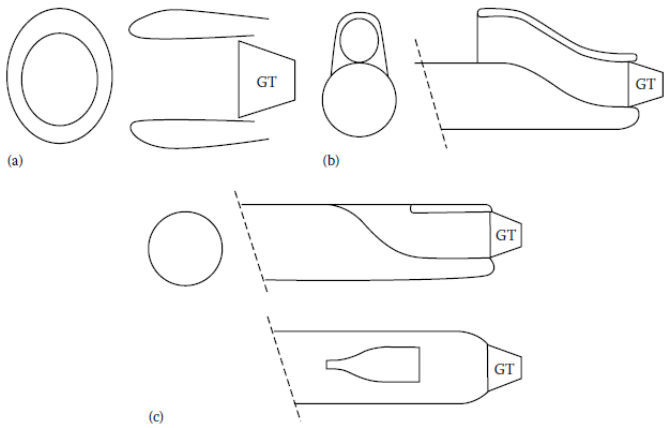

Figure 9.1: Air intakes: (a) standard, (b) integrated, (c) flush [9]

The main job of this piece is to convoy and prepare the fluid with the right speed and pressure to enter the first stage of the compressor. These operations need to be performed with the highest efficiency possible, to avoid big losses in pressure. We want the fluid, in this case the air, to be in the best conditions possible for the compressor, therefore there can't be sharp edges or fast variation in shape and diameter of the duct, in order to avoid flow separation and recirculation. For subsonic aircraft cruising at high speed the diffuser is usually a short circular or elliptical tube whose area gets bigger to slow the fluid down and prepare it for the compressor, so it has a standard divergent configuration. There are a lot of different geometrical possibilities as we can see from Figure 9.1. In our case the engine is embedded inside the fuselage to avoid aerodynamic problems and allow a clean shape, like most of UAV and small aircrafts. Therefore, an S-duct intake seems to be appropriate to be used. In this way we could have a little opening on the top or bottom of the aircraft, as done for APU in commercial aircrafts, and in some military model like the Lockheed Martin f-35.

To design our intake in an optimal way it has been decided to dimension it at cruise speed. Looking at Mach flight number (M_v=0.27) and seeing that it is in the low subsonic region, and that it is lower than the speed requested at the inlet of the LP-compressor (169.5 m/s), we conclude that our diffuser doesn't have to slow the fluid down, it has to accelerate it, so it will have a convergent geometry and will work as a nozzle instead. With this design we avoid flow separation thanks to favourable pressure gradients.

From previous calculations we know all the thermodynamical characteristics, outside of the intake and at its exit. Considering an isentropic flow we can calculate the area ratio, and accordingly the inlet area of our intake with the hypothesis that the entrance area of the compressor is equal to the exit area of the intake. We introduce a spillage factor $SF = \frac{\dot{m}_{engine}}{\dot{m}_{amb}} = 0.9$ knowing that some of the air won't enter the intake, thus we need a bigger intake to have the right mass flow rate.

$$\frac{A_{intake}}{A_2} = \frac{\pi_{intake}}{SF} \cdot \frac{M_{compr}}{M_a} \cdot \left(\frac{1 + \frac{k-1}{2} M_a^2}{1 + \frac{k-1}{2} M_{compr}^2} \right)^{\frac{k+1}{2(k-1)}} \tag{9.1}$$

With $A_2 = 0.0023m^2$ we obtain the following results:

- $\frac{A_{intake}}{A_2} = 2.0474$
- $A_{intake} = 0.0047m^2$

If we imagine having an intake shaped as half a circumference its radius would be 5.48 cm. For a rectangular shaped intake with a base of 10 cm the height of the intake would be 4.7cm.

9.2 Exhaust Nozzle

The nozzle role is to convert the remaining energy that the fluid has after having passed turbines and recuperator, into kinetic energy, producing thrust useful to push the aircraft. Since our plane provides thrust with the two fans driven by the electric motor, the majority of the enthalpic drop after the combustion chamber is done in the turbines, leaving a 0.6% of ΔH to be done in the nozzle. This will be a small convergent duct in which the flow can be considered isentropic, where the

fluid expands up to the ambient pressure. We will design the nozzle to be adapted at cruise altitude and speed.

Knowing the speed at the exit of the nozzle and all the parameters previously calculated, we manage to determine the nozzle exit area and the thrust generated as:

- $A_{nozzle} = \dot{m}_{comb}/(\rho \cdot V_{exit}) = 0.0067m^2$ (9.2)

- $T_{nozzle} = \dot{m}_{comb} * (V_{exit} - V_{cruise}) = 34.7\ N$ (9.3)

Imagining a circular exit for the exhaust gasses the radius of the nozzle will be 4.61 cm.

9.3 Material selection

For the intake, almost every material is good, since it works at low temperatures and doesn't have to sustain high mechanical loads or pressures. Composites made with injection moulding could be a good alternative to aluminium. A good material could be epoxy reinforced with fiberglass that gives good mechanical strength and low weight.

The exhaust nozzle seen the relatively high temperature to which it undergoes needs to be made of a high temperature and high resistance material. A nickel superalloy such as Inconel 625 will be used for its good mechanical characteristics already seen during the selection of the material for the combustion chamber and turbine.

Conclusions

A new type of engine for lightweight aircraft has been developed and designed. Having studied different setups the configuration with two heat exchangers has been chosen due to the important advantages they bring, improving both efficiencies and fuel consumption. The final configuration consists of: two parallel shafts on which two stages of compression and expansion are mounted, an intercooler to cool the flow down between the compressors, and a recuperator that manages to recover the high amount of energy still stored in the exhaust gasses that otherwise would be lost. In this way the combustion chamber doesn't have to do the entire work reducing consumptions and emissions. Finally, an electric current generator is keyed to the low-pressure shaft, supplying the electric motors whose fans produce the thrust. Every component used has been studied and designed thoroughly in order to gain maximum benefits. New advanced materials have been used to overcome weaknesses of commonly used ones that currently constrain the performance of the jet engines on the market. The solution implemented meets all the requirements set in the introduction exceeding by far the performance of an all-electric plane and allowing it to compete with the main players that nowadays own the commercial market of lightweight aircrafts. Moreover, this typology of engine thanks to his versatility can, with little modifications, be adapted to be used in drones for urban mobility, UAV's and all the cases where the distributed propulsion can be used. Additionally, using bigger turbomachines higher power could be reached opening new markets for this type of configuration.

I firmly believe that this concept could and will be the future for commercial aviation, changing the way we conceive aircrafts with completely innovative designs, and leading into a future where both performance and emissions control, do not exclude each other.

APPENDIX A: MATLAB

To understand and develop our engine a matlab code have been built so that we could see de various differences between the options studied in the shortest time as possible.

When developing the matlab code we wanted to assure the best accuracy possible at every step of the calculations, and for every different type of engine developed. To do so, we made sure that all the parameters that usually are taken constant but varies with temperature or altitude where modelled in the best way possible. Therefore, we implemented the following functions to add accuracy.

- Polytropic efficiency to calculate compressor and turbine efficiency
- Specific heat in function of temperature
- Same bat for after combustion
- Isa 76 model for atmosphere
- Aerodynamic model to calculate necessary power and trust

Aerodynamic model

In order to determine the aerodynamic parameters such as lift and drag, and the power necessary to fly the plane at a certain altitude and speed, we calculate the aerodynamic polars for cruise conditions where Lift=Weight and Thrust=Drag. Knowing the lift to drag ratio of the prototype made by Airbus, and considering it the maximum aerodynamic efficiency achievable, we determined lift and drag coefficients as such:

$$L = \frac{1}{2}\rho V^2 S\, Cl$$

$$D = \frac{1}{2}\rho V^2 S Cd \qquad with \qquad Cd = Cd0 + K \cdot Cl^2$$

$$therefore \qquad P_{required} = D \cdot V$$

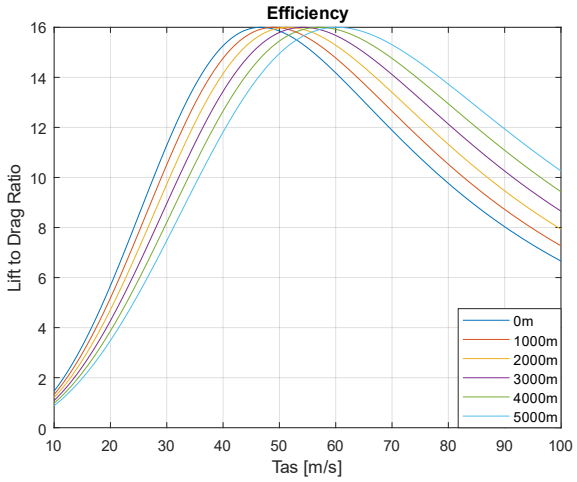

Figure A.0.1: Lift to drag ratio in function of speed and altitude

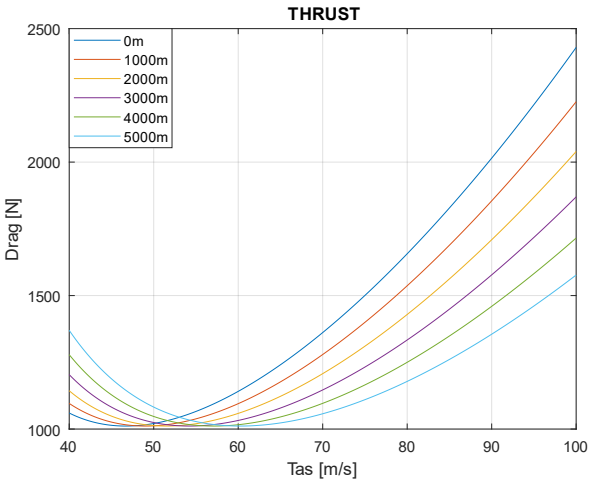

Figure A.0.2: Drag in function of speed and altitude

as can be seen from **Errore. L'origine riferimento non è stata trovata.** the aerodynamic efficiency considerably decreases after the maximum one, when we increase the flight speed. This is due to the fact that there is n important increase of drag at higher speeds. Moreover, the higher we fly the faster we need to be to get maximum efficiency. The Drag graph shows us the ideal speed at which we can fly with minimum resistance and therefore with less power needed. Ideally, we should cruise at speeds near to this one in order to have higher overall efficiencies. The last graph represents the power needed at a certain speed and altitude to sustain our cruise. Implementing the flight performance on our MATLAB code is useful to

have a clearer image of the aerodynamic performance of our aircraft and to get the most accurate results.

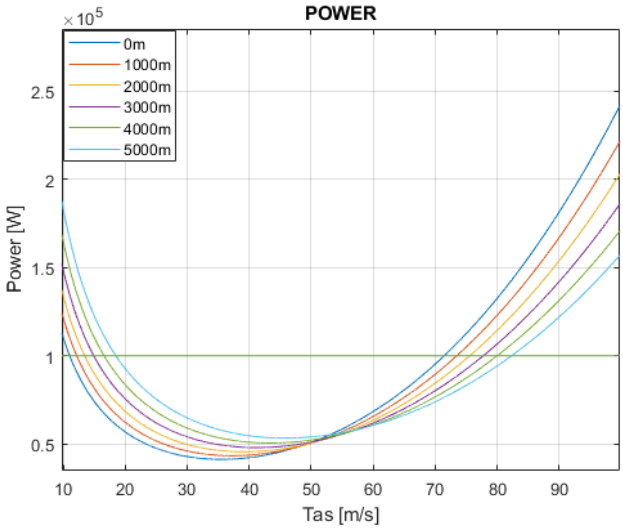

Figure A.0.3:Power in function of speed and altitude

Efficiencies

Every program made for this thesis has been developed considering the dependency of the efficiencies of the turbomachines from the pressure ratio and the gas constant. In particular it has been decided to set a fixed polytropic efficiency at 0.85 for both compressors and turbines and to calculate the isentropic efficiencies using the following formulas:

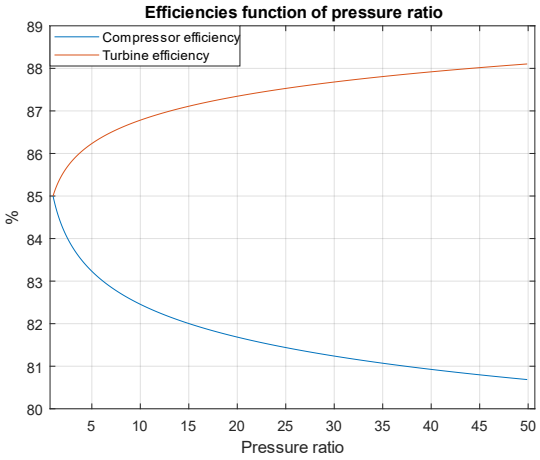

Figure A.0.4: efficiencies in function of pressure ratio

$$\eta_c = \frac{rp^{\frac{k-1}{k}} - 1}{rp^{\frac{k-1}{k \cdot \eta_{pol}}} - 1}$$

$$\eta_t = \frac{1 - er^{\frac{(k-1)\cdot\eta_{pol}}{k}}}{1 - er^{\frac{k-1}{k}}}$$

As can be seen from Figure A.0.4, there is a great variation of the efficiency with the pressure ratio in the range 0 to 10 which is the one we are most interested in. in a turbomachine a difference of 2% could mean a lot in term of energy produced or used therefore is important to take this as accurate as possible.
Other efficiencies such as pressure losses in combustion, mechanical efficiency of the shaft or energy conversion efficiency are decided after a thorough study of the elements currently on the market, averaging the various numbers without taking the best value.

Specific heat

One of the most important things that usually are taken constant but varies a lot with respect to the working temperature are the specific heats. Usually using ideal gasses with little variation of temperature there is no arm in taking them constant, but in a gas turbine where th delta T are higher, this could lead to errors greater than 5% tha propagates over the code could lead to huge differences in results. Specific heats are function of temperature and pressure, but it has been seen [], [] taking into account just the variation with temperature, results in an accurate estimate of their values. We report down here the empirical formula used and in figure [] the variation they have over time. Even the value of k, ratio between specific heat at constant pressure and volume varies with temperature, even if a little, it has been taken into account.

$$Cp(T) = 1000 \cdot [2.506 \cdot 10^{-11} \cdot T^2 + .454 \cdot T^{1.5} \cdot 10^{-7} - 4.246 \cdot 10^{-7} \cdot T + 3.162 \cdot 10^{-5} \cdot T^{0.5} + 1.3303 - 1.512 \cdot 10^{4} \cdot T^{-1.5} + 3.063 \cdot 10^{5} \cdot T^{-2} - 2.212 \cdot 10^{7} \cdot T^{-3}]$$

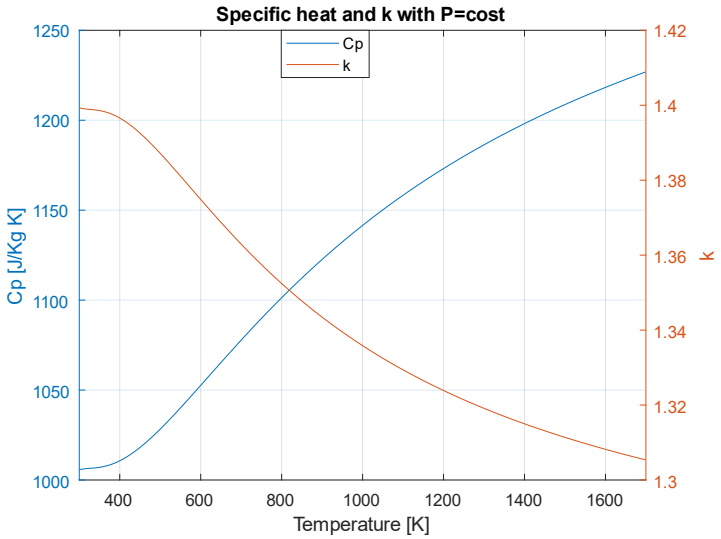

Figure A.0.5: specific heat f air in function of temperature

After the combustion chamber specific heat of air could not be used because the chemical components of the flow varies with the fuel used. In this case to determine the specific heats for all the fuels used we used a slightly different process, determining the cp of every chemical element in the combustion gasses (CO2, H2O, N2, …), mediating them in function of their quantities, to determine the overall cp. Here we report the variation with temperature of methane combusts.

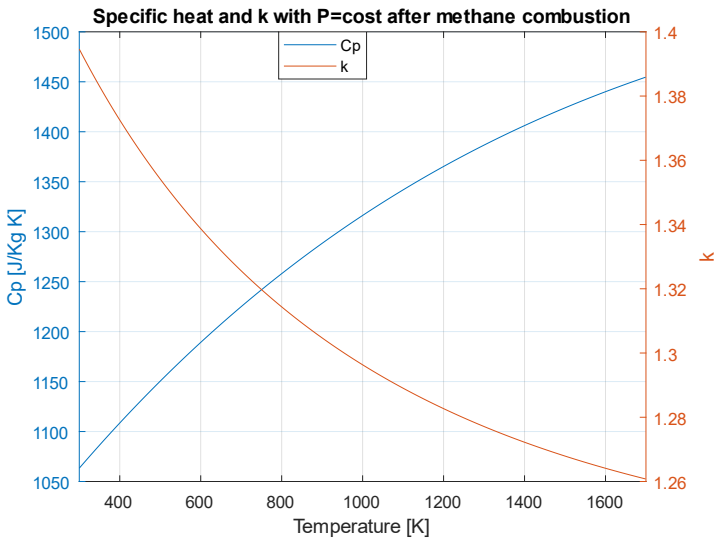

Figure A.0.6: specific heat of methane combusts in function of temperature

Model of the atmosphere

In order to have the correct pressure, temperature and density of the air entering our engine at different heights, hence to determine the permormance with high

accuracy, and atmospheric model has been implemented. We chose the International Standard Atmosphere ISA-76 because is the most used in aviation. The three major properties of a gas are calculated relying on a standard temperature at sea level of 25°C, a standard pressure of 101325 Pa and a standard density for the air of 1.225 Kg/m^3. Using a linear variation of temperature λ=-0.0065 K/m we determined the properties in function of altitude as:

$$T_a = T_0 + \lambda \cdot h$$

$$\rho_a = \rho_0 \left(1 + \frac{\lambda \cdot h}{T_0}\right)^{-1-\frac{g}{\lambda R}}$$

$$P_a = P_0 \left(1 + \frac{\lambda \cdot h}{T_0}\right)^{-\frac{g}{\lambda R}}$$

Bibliografia

[1] IATA, «Press release No 62: IATA Forecast Predicts 8.2 billion Air Travelers in 2037,» IAIA, 2018.

[2] X. ZHAO, Aero Engine Intercooling Conceptual design and experimental validation of an aero engine intercooler, Gothenburg, Sweden: CHALMERS UNIVERSITY OF TECHNOLOGY, 2016.

[3] BBC, «Denmark to make domestic flights fossil fuel free by 2030,» 2 January 2022. [Online]. Available: www.bbc.com/news/world-europe-59849898.

[4] D. o. S. a. M. Madison Xanders, *THE EARTHLY IMPACTS OF EXTRACTING LITHIUM.*

[5] P. e. a. Kolpakhchayan, « High speed generator for Gas Microturbine Installations,» *International journal of applied engineering,* vol. 12, n. 23, 2017.

[6] R. H. Aungier, Centrifugal compressors - A strategy for Aerodynamic Design and Analysis, 2000.

[7] S. A. Korpela, Principles of Turbomachinery, Wiley, 2011.

[8] P. W. R. J. a. W. D. S. Colin Osbosne, « AERODYNAMIC AND MECHANICAL DESIGN OF AN 8:1 PRESSURE RATIO CENTRIFUGAL COMPRESSOR,» NASA, 1975.

[9] A. E. El-Sayed, Aircraft propulsion and gas turbine engines Second Edition, Taylor & Francis, 2017 .

[10] A. Whitfield, «The Preliminary Design of Radial Inflow turbines,» *Journal of turbomachinery,* vol. 112, n. 57, 1990.

[11] R. H. Aungier, Turbine Aerodynamics: Axial-Flow and Radial-Inflow Turbine Design and Analysis, American Society of Mechanical Engineers, 2006.

[12] H. Kaya, «The application of ceramic-matrix composites to the automotive ceramic gas turbine,» *Composites Science and Technology ,* vol. 59, pp. 861-872, 1999.

[13] V. Bhandari, Design of Machine Elements, Mcgraw Hill Education, 2010.

[14] P. C. Hill P., Mechanics and Thermodynamics of Propulsion, 2/e, Pearson, 1991.

[15] S. JW., Sawyers Gas Turbine Engineering handbook, Turbomachinery Iternational, 1985.

[16] B. D. Lefebvre AH., Gas turbine combastion and alternative fuels and emissios, 2010.

[17] J. T. A. C. A. J. C. C. A. Adamou, «Design, simulation, and validation of additively manufactured,» *Energy Conversion and Management,* vol. 248, 2021.

[18] G. E. A. a. H. L. Mohamed Alalim Altaher, «Study of Biodiesel Emissions and Carbon Mitigation in Gas Turbine Combustor,» *American Journal of Engineering Research (AJER),* vol. 03, n. 11, pp. 290-298, 2014.

[19] K. R. G. S. J. Syed Ameer Basha, «A review on biodiesel production, combustion, emissions and performance,» *Renewable and Sustainable Energy Reviews,* vol. 13, pp. 1628-1634, 2009.

[20] A. G.-M. A. U.-R. J. B.-F. J.A. Alfaro-Ayala, «Use of bioethanol in a gas turbine combustor,» *Applied Thermal Engineering,* vol. 61, pp. 481-490, 2013.

[21] I.-N. z. 2. s. a. fuels, «www.iata.org/en/programs/environment/sustainable-aviation-fuels/,» [Online].

[22] M. S. Y. H. K. L. ,. C. W. Zhentao Liu, «Investigation of heat transfer characteristics of high-altitude intercooler for piston aero-engine based on multi-scale coupling method,» *International Journal of Heat and Mass Transfer,* vol. 156, n. 119898, 2020.

[23] X. H. W. X. Jun Cai, «An optimal design approach for the annular involute-profile cross wavy primary surface recuperator in microturbine and an application case study,» *Energy,* vol. 153, pp. 80-89, 2018.

[24] N. P. Kenneth E., «How to select Turbomachinery for your application,» Barber-Nichols Inc..